Title

Mutations in FGF17, IL17RD, DUSP6, SPRY4, and FLRT3 Are Identified in Individuals with Congenital Hypogonadotropic Hypogonadism

Journal

American Journal of Human Genetics, 92(5)

ISSN

0002-9297

Authors

Miraoui, Hichem
Dwyer, Andrew A
Sykiotis, Gerasimos P
et al.

Publication Date

2013-05-01

DOI

10.1016/j.ajhg.2013.04.008

Peer reviewed

Mutations in *FGF17*, *IL17RD*, *DUSP6*, *SPRY4*, and *FLRT3* Are Identified in Individuals with Congenital Hypogonadotropic Hypogonadism

Hichem Miraoui,[1,2] Andrew A. Dwyer,[1,2] Gerasimos P. Sykiotis,[2,3] Lacey Plummer,[2] Wilson Chung,[4] Bihua Feng,[2] Andrew Beenken,[5] Jeff Clarke,[6] Tune H. Pers,[7,8,9] Piotr Dworzynski,[7] Kimberley Keefe,[2] Marek Niedziela,[10] Taneli Raivio,[11] William F. Crowley, Jr.,[2] Stephanie B. Seminara,[2] Richard Quinton,[12] Virginia A. Hughes,[1,2] Philip Kumanov,[13] Jacques Young,[14] Maria A. Yialamas,[15] Janet E. Hall,[2] Guy Van Vliet,[16] Jean-Pierre Chanoine,[17] John Rubenstein,[6] Moosa Mohammadi,[5] Pei-San Tsai,[4] Yisrael Sidis,[1,2] Kasper Lage,[7,8,18,19,20] and Nelly Pitteloud[1,2,20,*]

Congenital hypogonadotropic hypogonadism (CHH) and its anosmia-associated form (Kallmann syndrome [KS]) are genetically heterogeneous. Among the >15 genes implicated in these conditions, mutations in *FGF8* and *FGFR1* account for ~12% of cases; notably, *KAL1* and *HS6ST1* are also involved in FGFR1 signaling and can be mutated in CHH. We therefore hypothesized that mutations in genes encoding a broader range of modulators of the FGFR1 pathway might contribute to the genetics of CHH as causal or modifier mutations. Thus, we aimed to (1) investigate whether CHH individuals harbor mutations in members of the so-called "*FGF8* synexpression" group and (2) validate the ability of a bioinformatics algorithm on the basis of protein-protein interactome data (interactome-based affiliation scoring [IBAS]) to identify high-quality candidate genes. On the basis of sequence homology, expression, and structural and functional data, seven genes were selected and sequenced in 386 unrelated CHH individuals and 155 controls. Except for *FGF18* and *SPRY2*, all other genes were found to be mutated in CHH individuals: *FGF17* (n = 3 individuals), *IL17RD* (n = 8), *DUSP6* (n = 5), *SPRY4* (n = 14), and *FLRT3* (n = 3). Independently, IBAS predicted *FGF17* and *IL17RD* as the two top candidates in the entire proteome on the basis of a statistical test of their protein-protein interaction patterns to proteins known to be altered in CHH. Most of the *FGF17* and *IL17RD* mutations altered protein function in vitro. *IL17RD* mutations were found only in KS individuals and were strongly linked to hearing loss (6/8 individuals). Mutations in genes encoding components of the FGF pathway are associated with complex modes of CHH inheritance and act primarily as contributors to an oligogenic genetic architecture underlying CHH.

Introduction

Congenital hypogonadotropic hypogonadism (CHH [MIM 146110]) due to gonadotropin-releasing hormone (GnRH) deficiency and/or resistance is a rare genetic disorder characterized by abnormal pubertal development and infertility.[1] CHH is often associated with anosmia and is then termed Kallmann syndrome (KS [MIM 308700, 147950, 244200, 610628, 612370, and 612702]), as well as with other phenotypes including unilateral renal agenesis, skeletal abnormalities, midline malformations, and hearing loss.[2] A number of genes are associated with congenital GnRH deficiency.[3] Nevertheless, <40% of individuals have been shown to harbor mutations in one or more of the >15 known genes. Most of the genes mutated in CHH encode receptor-ligand pairs (*GNRHR* [gonadotropin-releasing hormone receptor; MIM 138850] and *GNRH1* [gonadotropin-releasing hormone 1; MIM 152760]; *PROKR2* [prokineticin receptor 2; MIM 607123] and *PROK2* [prokineticin 2; MIM 607002]; *TACR3* [tachykinin receptor 3; MIM 162332] and *TAC3* [tachykinin 3; MIM 162330]; *KISS1R* [KISS1 receptor; MIM 604161] and *KISS1*

[1]Faculty of Biology and Medicine, University of Lausanne in collaboration with Service of Endocrinology, Diabetology, and Metabolism, Centre Hospitalier Universitaire Vaudois, Rue du Bugnon 7, Lausanne CH-1005, Switzerland; [2]Harvard Medical School Center of Excellence in Reproductive Endocrinology in collaboration with Reproductive Endocrine Unit, Massachusetts General Hospital, 55 Fruit Street, Bartlett Hall Extension, Fifth Floor, Boston, MA 02114, USA; [3]Division of Endocrinology and Metabolism, Department of Internal Medicine, University of Patras Medical School, Patras 26500, Greece; [4]Department of Integrative Physiology and Center for Neuroscience, University of Colorado, Boulder, CO 80309, USA; [5]Department of Biochemistry & Molecular Pharmacology, New York University School of Medicine, New York, NY 10016, USA; [6]Nina Ireland Laboratory of Developmental Neurobiology, Center for Neurobiology and Psychiatry, Department of Psychiatry, University of California, San Francisco, San Francisco, CA 94158-2324, USA; [7]Center for Biological Sequence Analysis, Technical University of Denmark, Lyngby 2800, Denmark; [8]Broad Institute of Harvard and MIT, Cambridge, MA 02142, USA; [9]Division of Endocrinology and Center for Basic and Translational Obesity Research, Boston Children's Hospital, Boston, MA 02114, USA; [10]Department of Pediatric Endocrinology and Rheumatology, Poznan University of Medical Sciences, Poznan 60-572, Poland; [11]Institute of Biomedicine (Physiology), University of Helsinki in collaboration with Children's Hospital, Helsinki University Central Hospital, Helsinki 00029, Finland; [12]Institute of Genetic Medicine, Newcastle University, Newcastle upon Tyne NE1 3BZ, UK; [13]Clinical Center of Endocrinology, Sofia Medical University, Sofia 1431, Bulgaria; [14]Service d'Endocrinologie et des Maladies de la Reproduction, Hôpital Bicêtre, Le Kremlin Bicêtre 94275, France; [15]Endocrine Division, Department of Medicine, Brigham & Women's Hospital, Boston, MA 02114, USA; [16]Endocrinology Service and Research Center, Centre Hospitalier Universitaire Sainte-Justine in collaboration with Factulty of Medicine, University of Montréal, Montréal QC H3T 1C5, Canada; [17]Endocrinology and Diabetes Unit, British Columbia Children's Hospital, University of British Columbia, Vancouver, BC V6H 3V4, Canada; [18]Pediatric Surgical Research Laboratories, Department of Molecular Biology and Analytical and Translational Genetics Unit, Department of Medicine, Massachusetts General Hospital, Boston, MA 02114, USA; [19]Novo Nordisk Foundation Center for Protein Research, University of Copenhagen, Copenhagen 2200, Denmark
[20]These authors contributed equally to this work
*Correspondence: nelly.pitteloud@chuv.ch
http://dx.doi.org/10.1016/j.ajhg.2013.04.008.

[KiSS-1 metastasis suppressor; MIM 603286]; and *FGFR1* [fibroblast growth factor receptor 1; MIM 136350] and *FGF8* [fibroblast growth factor 8; MIM 600483]), suggesting that multiple receptor-ligand-encoding gene networks are involved in the molecular pathology of the disease.

The discovery of mutations in *FGFR1* and *FGF8* in CHH[4,5] has demonstrated a previously unappreciated role of FGF8-FGFR1 signaling in GnRH neuron ontogeny. We have documented a lack of GnRH neurons in the hypothalamus of *Fgf8* hypopmorphic mice, which underscores the exquisite sensitivity of the GnRH neuronal population to FGF8 signaling.[5] Subsequent studies have established FGF8 as a critical morphogen for GnRH neuron fate specification, as well as for the development of the olfactory system.[6] Other tissues patterned by FGF8 include the ears, eyes, kidneys, and limbs,[7–10] all of which can be affected in CHH.[11]

KAL1 (Kallmann syndrome 1 sequence [MIM 300836]) and *HS6ST1* (heparan sulfate 6-O-sulfotransferase 1 [MIM 604846]), two genes known to be mutated in CHH, also encode important components of FGF8-FGFR1 signaling. *KAL1*, the first gene discovered to harbor mutations in KS,[12,13] encodes anosmin-1, which enhances FGF signaling by direct physical interactions with the FGFR-FGF-heparan sulfate proteoglycan (HSPG) complex on the cell surface.[14] *HS6ST1*, which encodes a heparan sulfotransferase enzyme, was identified as a gene mutated in CHH on the basis of a *C. elegans* study demonstrating that heparan 6-O-sulfation was required for anosmin-1 function in vivo.[15] The fact that multiple genes encoding components of the FGF pathway are already known to be mutated in CHH (e.g., *KAL1*, *HS6ST1*, *FGF8* and *FGFR1*) led us to hypothesize that a broader survey of the FGF network might uncover additional mutated genes.

Expression data from diverse organisms have identified a cluster of genes that are similarly expressed and regulated during development, and these are collectively referred to as "the *FGF8* synexpression group."[16–18] These genes not only show spatiotemporal expression patterns similar to that of *FGF8* but also specifically modulate the signaling efficiency of FGF8 through FGFR1 as enhancers or inhibitors (Table 1[16,18–36] and Figure 1A). We therefore considered five members of the *FGF8* synexpression group as candidate genes: interleukin 17 receptor D (*IL17RD* [MIM 606807]), dual specificity phosphatase 6 (*DUSP6* [MIM 602748]), sprouty homolog 2 (*Drosophila*) (*SPRY2* [MIM 602466]), and sprouty homolog 4 (*Drosophila*) (*SPRY4* [MIM 607984]), which are inhibitors, and fibronectin leucine rich transmembrane protein 3 (*FLRT3* [MIM 604808]), which is an enhancer[16–18] (Table 1 and Figure 1A). We also selected *FGF17* (fibroblast growth factor 17 [MIM 603725]) and *FGF18* (fibroblast growth factor 18 [MIM 603726]) because of their high homology to *FGF8* (with which they encode the so-called "FGF8 subfamily" of fibroblast growth factors [FGFs]),[37] their coexpression with *Fgf8* in the olfactory placode, and their shared ability to signal through FGFR1c[37] (Table 1 and Figure 1A).

Thus, the primary objective of this study was to investigate whether CHH individuals harbor mutations in genes encoding members of the extended FGF8-FGFR1 network. A secondary objective was to validate the ability of a bioinformatics tool on the basis of protein-protein interactome data to identify high-quality candidate genes and to prioritize them for experimental confirmation.

Subjects and Methods

Subjects

CHH was diagnosed and classified as KS or normosmic idiopathic hypogonadotropic hypogonadism (nIHH) according to standard criteria.[38] A cohort of 386 CHH individuals included 199 KS individuals (152 men and 47 women) and 187 nIHH individuals (140 men and 47 women). Several CHH probands harbored mutations in genes previously identified to be associated with nIHH and/or KS: *FGFR1* (n = 34 individuals), *KAL1* (n = 17), *FGF8* (n = 5), *HS6ST1* (n = 7), *PROKR2* (n = 14), *PROK2* (n = 4), *GNRHR* (n = 16), *GNRH1* (n = 2), *KISS1R* (n = 5), *KISS1* (n = 1), *NSMF* (NMDA receptor synaptonuclear signaling and neuronal migration factor, formerly known as *NELF* [MIM 608137]) (n = 4), *TAC3R* (n = 19), and *TAC3* (n = 1).[15,39–42] Also included was a control group of 155 unaffected subjects of European descent (83 men and 72 women) with normal reproductive function. The study was approved by the human research committee of Massachusetts General Hospital, and all subjects provided written informed consent prior to participation.

DNA Sequencing

Genomic DNA was extracted from peripheral-blood samples. The coding exons and proximal introns (≥15 bp from splice sites) of *FGF17* (five exons), *FGF18* (five exons), *IL17RD* (13 exons), *DUSP6* (three exons), *SPRY2* (two exons), *SPRY4* (two exons), and *FLRT3* (one exon) were amplified by PCR and determined by direct sequencing. Each gene's sequence was identified with the use of the UCSC and ENSEMBL genome databases. All DNA variants were found on both DNA strands and were confirmed in a separate PCR. Genes and proteins are described according to HGVS nomenclature. A variant was considered a mutation if it had a minor allele frequency (MAF) < 1% in unaffected controls (which includes "disease-only" variants with MAF = 0% in controls) and in the 1000 Genomes data set and if it altered a conserved amino acid or/and was predicted to cause loss of function by at least one prediction program (PolyPhen-2,[43] SIFT,[44] PMut,[45] or Mutation Taster[46] for missense variants and NNsplice[47] for splice-site variants). When a mutation was shown to impact protein function in in vitro studies, it was considered "functional."

Candidate-Gene Prioritization by Interactome-Based Affiliation Scoring

We applied a bioinformatrics method to discover and/or prioritize CHH candidate genes. The algorithm determines whether the interaction between a candidate protein (Cp) and a set of phenotype-causing proteins (PCPs) involved in a phenotype (F) is significant, contingent on the pattern of interactions observed between PCPs in a cross-validation step. A series of permutation procedures are used for ensuring that the interaction data and results are not confounded by biases or errors in the interactome data. If the

Table 1. CHH Candidate Genes Associated with the FGF8 Network

Gene	RefSeq Transcript	Chromosomal Location	Protein Size (aa)	Rationale for Selection		Expression in Mice[a]		Mouse Knockout Phenotype	Human Disease	References
				FGF8 Synexpression Member	Homology to *FGF8*	Olfactory Placode (E9.5–E11.5)	Hypothalamus (Adult)			
FGF17	NM_003867.2	8p21	216	–	+	+	+	medial cerebellar defects, frontal cortex anomalies	KS, nIHH	this study, Bachler and Neubüser,[19] Cholfin and Rubenstein,[20] Topp et al.,[21] and Xu et al.[22]
FGF18	NM_003862.2	5q34	207	–	+	+	–	craniofacial defects, abnormal limb development	–	Bachler and Neubüser,[19] Liu et al.,[23] and Ohbayashi et al.[24]
IL17RD	NM_017563.3	3p14.3	739	+	–	+	+	hearing defect, cerebellum anomalies	KS	this study, Fürthauer et al.,[16] Tsang et al.,[18] and Abraira et al.[25]
SPRY2	NM_005842.2	13q31.1	315	+	–	+	+	craniofacial defects, hearing defects	–	Fürthauer et al.,[16] Mailleux et al.,[26] de Maximy et al.,[27] and Shim et al.[28]
SPRY4	NM_030964.3	5q31.3	322	+	–	+	+	craniofacial defects, abnormal limb development	KS, nIHH	this study, Fürthauer et al.,[16] de Maximy et al.,[27] Shim et al.,[28] Taniguchi et al.,[29] and Leeksma et al.[30]
DUSP6	NM_001946.2	12q22–q23	381	+	–	+	+	craniofacial defects, hearing defects	KS, nIHH	this study, Dickinson et al.,[31] Li et al.,[32] and Vieira and Martinez[33]
FLRT3	NM_198391.2	20p11	649	+	–	+	+	abnormal neural tube	KS	this study, Böttcher et al.,[34] Maretto et al.,[35] and Robinson et al.[36]

Abbreviations are as follows: nIHH, normosmic idiopathic hypogonadotropic hypogonadism.
[a]Allen Brain Atlas and Brain Gene Expression Map databases.

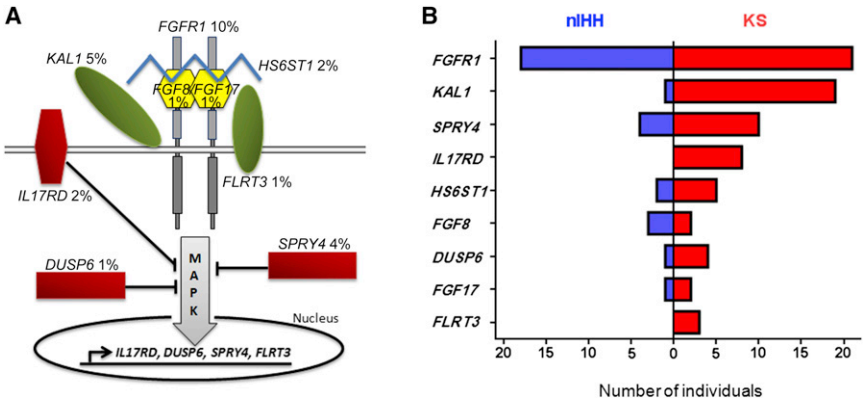

Figure 1. FGF-Network-Associated Genes Harbor Mutations in CHH Individuals
(A) A simplified schematic of the FGF pathway includes frequencies of mutations identified in CHH individuals. *KAL1* and *FLRT3*, encoding enhancers of FGF signaling, are shown in green; *IL17RD*, *DUSP6*, and *SPRY4*, encoding inhibitors, are in red; *HS6ST1*, encoding the HS-modifying enzyme, is in blue; *FGF8* and *FGF17*, encoding ligands, are in yellow; and *FGFR1*, encoding the receptor FGFR1, is in gray.
(B) Number of nIHH and KS individuals with mutations in each gene.

interaction between a Cp and the PCPs is significant, a Cp is determined to be associated with the F on the basis of its interactome; hence, we named the method interactome-based affiliation scoring (IBAS). Interactome data come from a well-established human protein interaction network (InWeb) of ~430,000 protein-protein interactions among 12,507 human proteins (InWeb[48–50]).

In this work, the PCPs are 14 proteins encoded by genes known to be involved in GnRH deficiency: *GNRH1*, *GNRHR*, *PROK2*, *PROKR2*, *KAL1*, *FGF8*, *FGFR1*, *TAC3*, *TACR3*, *KISS1*, *KISS1R*, *HS6ST1*, *CHD7* (chromodomain helicase DNA binding protein [MIM 608892]), and *PCSK1* (proprotein convertase subtilisin/kexin type 1 [MIM 162150]). First, IBAS was trained, parameter optimized, and validated on this set of known PCPs for the identification of the optimal set of parameters that could predict the PCPs among random proteins. In a standard leave-one-out cross-validation, the PCPs predicted each other with an area under the receiver-operating-characteristic curve of 0.8 ($p < 0.002$ with a permutation test). This allowed all candidates (i.e., 12,493 proteins covered by interaction data, excluding PCPs 1–14 in InWeb) to be scored and ranked, and permutation tests were used for determining the significance of the observed scores. IBAS will be presented in a separate paper in fuller detail, including a discussion of confounding factors, permutation strategies, and applications to data types, such as next-generation sequencing (K. Lage, unpublished data).

Functional Analyses of *IL17RD* Mutations

The ability of altered IL17RD proteins to inhibit FGF8 signaling was assessed in human embryonic kidney (HEK) 293 cells. The long form of human IL17RD-encoding cDNA (RefSeq accession number NM_017563) was subcloned into vector pcDNA3.1(+) (Invitrogen, Carslbad, CA, USA), and altered proteins were generated by site-directed mutagenesis. HEK293 cells were transiently transfected in 24-well plates at 40% confluency with 5 ng wild-type (WT) FGFR1c and 20 ng WT or altered IL17RD together with 5 ng AP-1 luciferase reporter (Stratagene, La Jolla, CA) and 170 ng empty vector (EV) with the use of FuGene6 reagent (Roche Diagnostics). AP-1 is activated by the mitogen-activated protein kinase (MAPK) downstream of FGFR1.[51] We avoided using constitutively active internal control reporters (such as pRL-TK or pRL-SV40) to correct for variations in transfection efficiency because they are responsive to FGFs.[52] Instead, experiments were performed in quadruplicate and repeated five times. After serum starvation, cells were treated with 0.2 nM FGF8b for 16 hr in serum-free medium. Data were normalized to the FGF8-treated EV response, and the mean values from five independent experiments were compared between each altered and WT protein with a Student's t test. Data are presented as the mean ± SEM.

Protein Expression and Glycosylation Analysis

To evaluate the potential effect of the mutations on IL17RD synthesis and folding, we assayed total-protein expression and glycosylation as previously described[52] with minor modifications. In brief, HEK293T cells were transiently transfected with 50 ng of C-terminal HA-tagged WT or mutated IL17RD-encoding cDNA and processed as reported. For immunoblot analysis, we used an HA primary antibody (1:2,000; Sigma-Aldrich, Saint Louis, MO, USA) and a rabbit anti-mouse horseradish-peroxidase-conjugated secondary antibody (1:20,000, Invitrogen). Endoglycosidase experiments were repeated three times, and protein expression and maturation levels were compared between each altered and WT protein with a Student's t test. Data are presented as the mean ± SEM.

Cell-Surface Expression

Expression of WT or altered IL17RD at the cell surface was quantified with an antibody-binding assay as previously described[52] with minor modifications. In brief, COS-7 cells were transiently transfected with 125 ng of N-terminal Flag-tagged WT or altered IL17RD. Cells were incubated with Flag antibody (1:1,000) and [^{125}I]-rabbit anti-mouse IgG (300,000 cpm/well; Perkin Elmer, Whaltham, MA, USA) and processed as previously reported.[52] Experiments were performed in quadruplicate and repeated four times. Specific cell-surface expression of altered IL17RD proteins was compared to that of the WT with a Student's t test. Data are presented as the mean ± SEM.

Functional Analyses of *FGF17* Mutations

Expression and Purification of WT and Altered FGF17 Ligands

Bacterially expressed WT FGF17 and p.Ile108Thr, p.Arg177His, and p.Asn187Ser altered FGF17 were refolded in vitro and purified by heparin affinity chromatography; size-exclusion chromatography was subseqntly performed at 4°C according to a published protocol.[5] The purification yield of the p.Ile108Thr altered protein was significantly less than that of the WT as a result of its precipitation during refolding and purification; this is in agreement with the prediction that the p.Ile108Thr substitution destabilizes the β-trefoil core of FGF17.

Surface-Plasmon-Resonance Spectroscopy

Physical interactions between the ligand-binding region (D2-D3 fragment) of human FGFR1c and WT or p.Arg177His altered FGF17 were analyzed by surface-plasmon-resonance (SPR) spectroscopy with a BIAcore 2000 system (GE Healthcare) as previously described.[37] WT FGF17, p.Arg177His altered FGF17, and FHF1b

(negative control) were immobilized onto separate flow channels of a research-grade CM5 biosensor chip (GE Healthcare) with the use of an amine coupling kit. In brief, carboxymethyl groups of the CM5 chip were activated by injection of 35 μl of a freshly prepared mixture of 0.05 M N-hydroxysuccinimide and 0.2 M N-ethyl-N-(dimethyaminopropyl) carbodiimide at a 5 μl/min flow rate. Thereafter, 5 μg/ml solutions of WT and p.Arg177His altered FGF17 or FHF1b in HBS-EP buffer (0.01 M HEPES, pH 7.4, 150 mM NaCl, 3 mM EDTA, 0.005% Surfactant P20) were passed over separate channels of the activated chip until 2,100 response units of WT or p.Arg177His altered FGF17 or 1,200 response units of FHF1b were immobilized. Unreacted sites on the chip surface were then blocked by injection of 35 μl of 1 M solution of ethanolamine. Increasing concentrations (100 nM to 3.2 μM) of the analyte (D2-D3 fragment of FGFR1c) were prepared in HBS-EP buffer and were passed over the channels containing the immobilized ligands at 50 μl/min, and the association phase of FGF17-FGFR1c interaction was monitored for 180 s. Thereafter, HBS-EP buffer was passed over the chip for 180 s for observation of the dissociation phase. Between analyte injections, the sensor surface was regenerated by 35 μl of 2.5 M NaCl in 5 mM HEPES (pH 7.5). Sensorgrams were processed in BIAevaluation software v.4.1.1.

Cell-Based Assays

FGF17-stimulated signaling activity was assessed in L6 myoblast cells as previously described.[5,53] In short, cells were transiently transfected with WT or altered FGFR1c expression vector in combination with the osteocalcin-FGF-response-element luciferase reporter. Cells were treated with increasing doses of WT or altered FGF17 and assayed for luciferase activity as described. The data were plotted and fitted with four-parameter sigmoidal dose-response curves with Prism software (version 5; GraphPad). Transfection experiments were performed in triplicate and repeated three times. Individual experiments were expressed as a percentage of the WT, and the mean maximal activity from three independent experiments was compared to that of the WT by a Student's t test. Data are presented as the mean ± SEM.

Mouse Studies

Mice were housed and handled in accordance with the Institutional Animal Care and Use Committee of the University of Colorado at Boulder. Mice homozygous for a hypomorphic *Fgf8* allele[54] and WT controls were obtained from the breeding of heterozygotes. For double GnRH and IL17RD immunohistochemistry (IHC), embryonic day (E) 10.5–E12.5 embryos were removed and fixed by immersion in 4% paraformaldehyde for 6 hr, cryoprotected in 30% sucrose, and cut on a cryostat. Thaw-mount sections (20 μm) were collected and processed for IHC with rabbit anti-GnRH antiserum LR5 (gift from R. Benoit, Montreal General Hospital) followed by goat anti-Il17rd antiserum (R&D Systems, Minneapolis, MN, USA). Secondary antibodies conjugated with different fluorophores were used for fluorescence labeling. For single GnRH IHC, E13.5 embryos and postnatal day (P) 0 brains were fixed, cryoprotected and sectioned as above, and processed as described.[55] *Fgf17* whole-mount RNA in situ hybridization (WM-ISH) was performed on *Fgf8* hypomorphic and WT mice as described[56] with a 679 nt digoxigenin-labeled *Fgf17* antisense riboprobe.

Assessment of Oligogenicity

In the same individual, the simultaneous presence of mutations in different disease-associated genes (oligogenicity) was evaluated for all subjects of European descent (350 CHH individuals and 155 controls) as described previously.[39] Each subject was scored as to the total number of alleles harboring mutations. In subjects with more than a single allele with such mutations (biallelic or triallelic), it was further noted whether these mutations were on alleles of the same or different genes (monogenic or oligogenic, respectively) by the sequencing of individual alleles after the cloning of PCR amplicons encompassing the mutations in the pTOPO vector (Invitrogen). Oligogenicity was compared between CHH individuals and controls by a Fisher's test.

Results

FGF17, *IL17RD*, *DUSP6*, *SPRY4*, and *FLRT3* Harbor Mutations in CHH Individuals

We sought mutations by Sanger sequencing in genes belonging to the *FGF8* subfamily (*FGF17* and *FGF18*) and the *FGF8* synexpression group (*IL17RD*, *DUSP6*, *SPRY2*, *SPRY4*, and *FLRT3*) among 386 CHH probands (199 KS and 187 nIHH) and 155 controls. This functional candidate-gene approach was fruitful in yielding mutations among CHH probands in five of seven genes screened, and each individual gene contributed to a small percentage of cases (1%–4%) (Figure 1A and Table S1, available online). The genotypes and phenotypes of the CHH probands with mutations in *FGF17*, *IL17RD*, *DUSP6*, *SPRY4*, and *FLRT3* are summarized in Table 2; individuals carrying functionally characterized mutations in *FGF17* or *IL17RD* are presented in more detail below. Taking into account the previously described CHH-associated mutated genes that also belong to the *FGF8* module (*FGFR1*, *FGF8*, *KAL1*, and *HS6ST1*) (Tables S1 and S2), 23% (91/386) of CHH probands harbored mutations in at least one gene associated with the FGF network; 74% (67/91) of these had KS (Figure 1B).

IBAS Identifies *IL17RD* and *FGF17* as the Top CHH Candidate Genes

A bioinformatics method (IBAS) was independently utilized for identifying and prioritizing candidate CHH genes. The protein-protein interactome-based algorithm trained on the set of proteins encoded by the genes known to be mutated in CHH identified 35 proteins with a posterior probability [PP] score > 0.32 (Figure 2 and Table S5). We estimated the empirical probability of observing a PP ≥ 0.32 by ranking all 12,507 proteins in InWeb by using 500 random models to obtain a null distribution of random PPs; this indicated that a PP ≥ 0.32 is highly significant at $p < 1/500 = 0.002$. In a comparison between the ranked list and the sequencing results, it was notable that IL17RD had the highest PP and that FGF17 had the second-highest PP; in constrast, DUSP6, SPRY4, and FLRT3 were not among the top 35 proteins. Therefore, *IL17RD* and *FGF17* were selected among the five mutation-harboring genes for functional characterization of the mutants and further experimental validation.

Table 2. Genotypes and Phenotypes of 30 CHH Probands with FGF8-Network-Associated Gene Mutations Identified Herein

Family	Proband Dx	Sex	Inheritance	Puberty	Hearing Loss	Abnormal Dentition	Low Bone Mass	Gene(s)	Nucleotide Change(s)	Amino acid Change(s)
1	KS	male	S	A	–	–	–	*IL17RD*	c.392A>C	p.Lys131Thr
2	KS	male	F	P	–	+	–	*IL17RD*	c.392A>C	p.Lys131Thr
3	KS	female	S	A	+	–	+	*IL17RD*	c.485A>G	p.Lys162Arg
4	KS	female	S	A	+	–	–	*IL17RD*	c.916C>T[a]	p.Pro306Ser
5	KS	female	F	A	+	+	+	*IL17RD*	c.1136A>G	p.Tyr379Cys
								FGFR1	c.1042G>A	p.Gly348Arg
6	KS	male	F	A	+	–	+	*IL17RD*	c.1403C>T	p.Ser468Leu
7	KS	male	F	A	+	+	–	*IL17RD*	c.1730C>A[a]	p.Pro577Gln
8	KS	male	F	A	+	–	–	*IL17RD*	c.2204C>T	p.Ala735Val
								KISS1R	c.581C>A	p.Ala194Asp
9	KS	female	F	A	–	–	+	*FGF17*	c.323T>C	p.Ile108Thr
								FLRT3	c.290A>G	p.Glu97Gly
									c.431G>T[a]	p.Ser144Ile
								HS6ST1	c.917G>A[a]	p.Arg306Trp
								FGFR1	c.749G>A	p.Arg250Gln
10	nIHH	male	S	A	–	–	+	*FGF17*	c.530G>A	p.Arg177His
11	KS	male	S	A	–	–	–	*FGF17*	c.560A>G	p.Asn187Ser
12	nIHH	female	F	A	–	+	–	*DUSP6*	c.229T>A	p.Phe77Ile
13	KS	male	F	A	–	+	–	*DUSP6*	c.545C>T	p.Ser182Phe
								FGFR1	c.2075A>G	p.Glu692Gly
14	KS	male	F	A	–	–	–	*DUSP6*	c.566A>G	p.Asn189Ser
15	KS	female	S	A	–	–	+	*DUSP6*	c.566A>G	p.Asn189Ser
								SPRY4	c.722C>A	p.Ser241Tyr
16	KS	female	S	A	+	–	+	*DUSP6*	c.1037C>T	p.Thr346Met
								SPRY4	c.722C>A	p.Ser241Tyr
17	nIHH	male	S	NA	–	–	–	*SPRY4*	c.46G>A	p.Val16Ile
18	KS	male	S	A	+	–	–	*SPRY4*	c.299C>T	p.Thr100Met
19	nIHH	male	F	P	–	–	–	*SPRY4*	c.313G>A	p.Asp105Asn
20	KS	male	S	A	–	–	–	*SPRY4*	c.530A>G	p.Lys177Arg
21	KS	male	S	A	–	+	–	*SPRY4*	c.530A>G	p.Lys177Arg
22	KS	male	S	A	–	–	–	*SPRY4*	c.530A>G	p.Lys177Arg
23	KS	male	F	A	+	–	–	*SPRY4*	c.530A>G	p.Lys177Arg
24	KS	male	S	A	–	–	–	*SPRY4*	c.626G>A	p.Cys209Tyr
25	KS	male	S	A	–	–	–	*SPRY4*	c.722C>A	p.Ser241Tyr
								FGFR1	c.1447C>A	p.Pro483Thr
26	nIHH	female	F	A	–	+	+	*SPRY4*	c.722C>A	p.Ser241Tyr
27	nIHH	male	S	A	–	–	+	*SPRY4*	c.841G>A	p.Val281Met
28	nIHH	female	S	P	–	–	–	*SPRY4*	c.910G>A	p.Val304Ile

(*Continued on next page*)

Table 2. *Continued*

Family	Proband Dx	Sex	Inheritance	Puberty	Hearing Loss	Abnormal Dentition	Low Bone Mass	Gene(s)	Nucleotide Change(s)	Amino acid Change(s)
29	KS	female	F	A	+	–	+	*FLRT3*	c.205C>A	p.Gln69Lys
								FGFR1	c.2008G>A	p.Glu670Lys
30	KS	male	F	P	–	–	–	*FLRT3*	c.1016A>G	p.Lys339Arg

Abnormal dentition includes abnormal development of teeth or crowded, extra, or missing teeth. Low bone mass includes osteopenia, osteoporosis, or fractures. Abbreviations are as follows: Dx, diagnosis; S, sporadic; F, familial; P, partial; A, absent (absent puberty is defined as testicular volume ≤ 3 ml or primary amenorrhea at presentation); and NA, not assessed.
[a]Homozygous mutation.

Mutations in *IL17RD* Are Associated with KS and a High Frequency of Hearing Loss

Clinical data on the eight unrelated CHH probands harboring missense heterozygous and homozygous *IL17RD* mutations are summarized in Table 2 and Figure 3B. Notably, all have KS; 7/8 have absent puberty, and 6/8 exhibit congenital hearing loss, which is unilateral in most (5/8). In fact, the two probands without hearing loss (II-1 in F1 and II-2 in F2) carry the same c.392A>C (p.Lys131Thr) mutation (Figure 3B). In two pedigrees with hearing loss, the probands (II-4 in F4 and II-2 in F7) carry homozygous *IL17RD* mutations; the parents, who are known or assumed to carry one mutant allele, display neither hearing loss nor hypogonadism (Figure 3B). In two other pedigrees, the probands (II-2 in F5 and II-3 in F8), who are the only family members with hearing loss, demonstrate apparently oligogenic inheritance: a heterozygous *IL17RD* mutation plus a heterozygous *FGFR1* or *KISS1R* mutation. Pedigree F5 indicates that the heterozygous *IL17RD* mutation is insufficient to cause hearing loss, given that the proband's mother (I-2), who carries the *IL17RD*, but not the *FGFR1*, mutant, has normal hearing. Lastly, hearing loss does not cosegregate with the *IL17RD* mutation in pedigree F6, given that the proband's fraternal twin (II-4) has hearing loss without the mutation and their mother (I-2) carries the mutation but has normal hearing (Figure 3B). Collectively, these data indicate that *IL17RD* mutations are strongly associated with KS and hearing loss; however, one allelic defect is most likely not sufficient, meaning that additional affected alleles in the same and/or other genes must be present to create the phenotype of KS with hearing loss.

Functional Characterization of the CHH-Associated *IL17RD* Mutations

All *IL17RD* mutations were predicted to be pathogenic in three out of four prediction programs; the only exception was c.485A>G (p.Lys162Arg), which was predicted to cause loss of function by only one program (Table S1). Because IL17RD is an inhibitor of FGF signaling (Figure 1A), loss of IL17RD function is expected to lead to higher FGF-pathway activity. The functional effect of the identified mutations (Figure 3A) on FGF signaling was tested in a cell-based reporter-gene assay. Cells expressing WT FGFR1c alone elicited a 3-fold increase in the activity of the AP-1 luciferase reporter when treated with FGF8b (Figure 3C), whereas, similarly to untreated cells, cells coexpressing WT IL17RD exhibited markedly lower activity (70% inhibition). For a negative control, we employed a truncated IL17RD form (Δ326) that lacks the entire intracellular domain[57] and fails to inhibit FGF8 downstream signaling. The p.Lys131Thr, p.Pro306Ser, and p.Ser468Leu altered IL17RD proteins inhibited FGF8 signaling to a significantly lesser degree than did WT IL17RD (89%, 67%, and 32% relative to WT, respectively; $p < 0.05$) (Figure 3C), indicating loss of function; the p.Tyr379Cys and p.Pro577Gln altered proteins also demonstated reduced inhibitory activity (75% and 82% relative to WT, respectively), which approached significance ($p = 0.06$) (Figure 3C). The p.Lys162Arg and p.Ala735Val altered proteins behaved similarly to WT IL17RD in this assay (Figure 3C). Overall expression levels of the altered proteins were similar to that of the WT (Figures S2A and S2B). The mature IL17RD fraction of p.Lys131Thr and p.Lys162Arg was increased compared to that of the WT (122% and 105%, respectively; $p < 0.05$) (Figure S2C), whereas that of p.Ser468Leu was decreased (80% relative to WT; $p < 0.05$). The p.Lys131Thr, p.Lys162Arg, and p.Ala735Val altered proteins all exhibited significantly decreased cell-surface expression than did the WT (~15%, $p < 0.05$), whereas that of the p.Ser468Leu altered protein was ~50% of that of the WT ($p < 0.05$) (Figure S2D). The other altered proteins (p.Pro306Ser, p.Tyr379Cys, and p.Pro577Gln) had cell-surface expression similar to that of the WT (Figure S2D).

FGF8 Is Required for IL17RD Localization in the Olfactory Placode

To link IL17RD to GnRH neuron fate specification and migration, we investigated the localization patterns of IL17RD and GnRH in the nasal region of mouse embryos at E10.5–E12.5. IL17RD immunoreactivity was highest in the E10.5 epithelium of the developing olfactory placode, where FGF8 is present, whereas it was much milder in the mesenchyme (Figure 3D, left panel).[19] IL17RD localized to the perinuclear compartment of the cell (Figure 3D, right panel).[58] At E12.5, IL17RD reactivity was no longer detectable in the olfactory epithelium (Figure 3E, lower inset) but

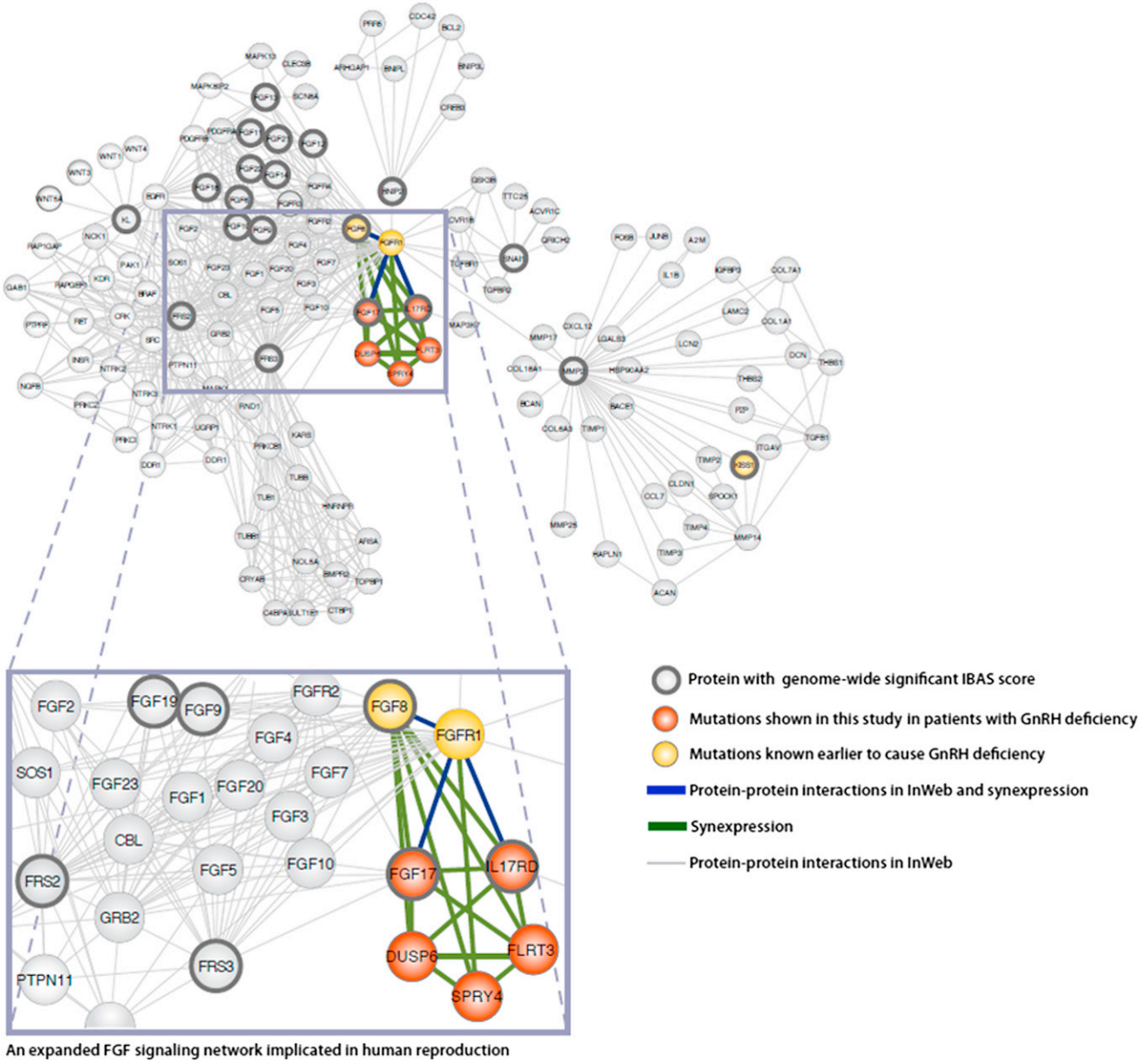

Figure 2. An Integrated FGF Signaling Network of Protein-Protein Interactions and Gene-Synexpression Data Implicated in Human Reproduction

Proteins identified by IBAS to significantly interact with FGF8 and FGFR1 are shown in this network. On the basis of high-quality protein-protein interaction data from InWeb, 17 proteins have genome-wide-significant IBAS scores as a result of their interaction patterns with the FGFR1-FGF8 receptor-ligand pair. Moreover, five proteins (FGF17, IL17RD, DUSP6, SPRY4, and FLRT3) are synexpressed with FGF8 and FGFR1 during development. IL17RD and FGF17 are the top-scoring candidates among 12,507 proteins in InWeb.

was detected in the septal area and in the midbrain-hindbrain junction (Figure 3E). IL17RD was undetectable in the brain of *Fgf8* hypomorphic embryos. We also evaluated localization patterns of IL17RD and GnRH at E11.5, when GnRH neurons begin migrating from the olfactory placode to the developing olfactory bulb. In these mice, IL17RD levels were dramatically decreased overall relative to E10.5 mice, yet IL17RD was present in a few GnRH neurons (Figure S2E). Cumulatively, these studies suggest that IL17RD might have a role in the early stages of GnRH neuron fate specification.

A KS-Associated *FGFR1* Mutation Implicates FGF17 as a Ligand Involved in GnRH Biology

FGF17 shares 61% overall sequence identity with FGF8b, signals through FGFR1c, and exhibits the same receptor-binding-specificity profile as FGF8b.[37] The association between *FGF8b* mutations and KS was based on the discovery of a heterozygous *FGFR1c* mutation, c.1025T>C (p.Leu342Ser), in a KS individual in whom FGF8b binding was abolished in transfected cells.[53] The p.Leu342Ser altered FGFR1c maps to a hydrophobic groove that is conserved in the D3 of FGFR1c, FGFR2c, FGFR3c, and

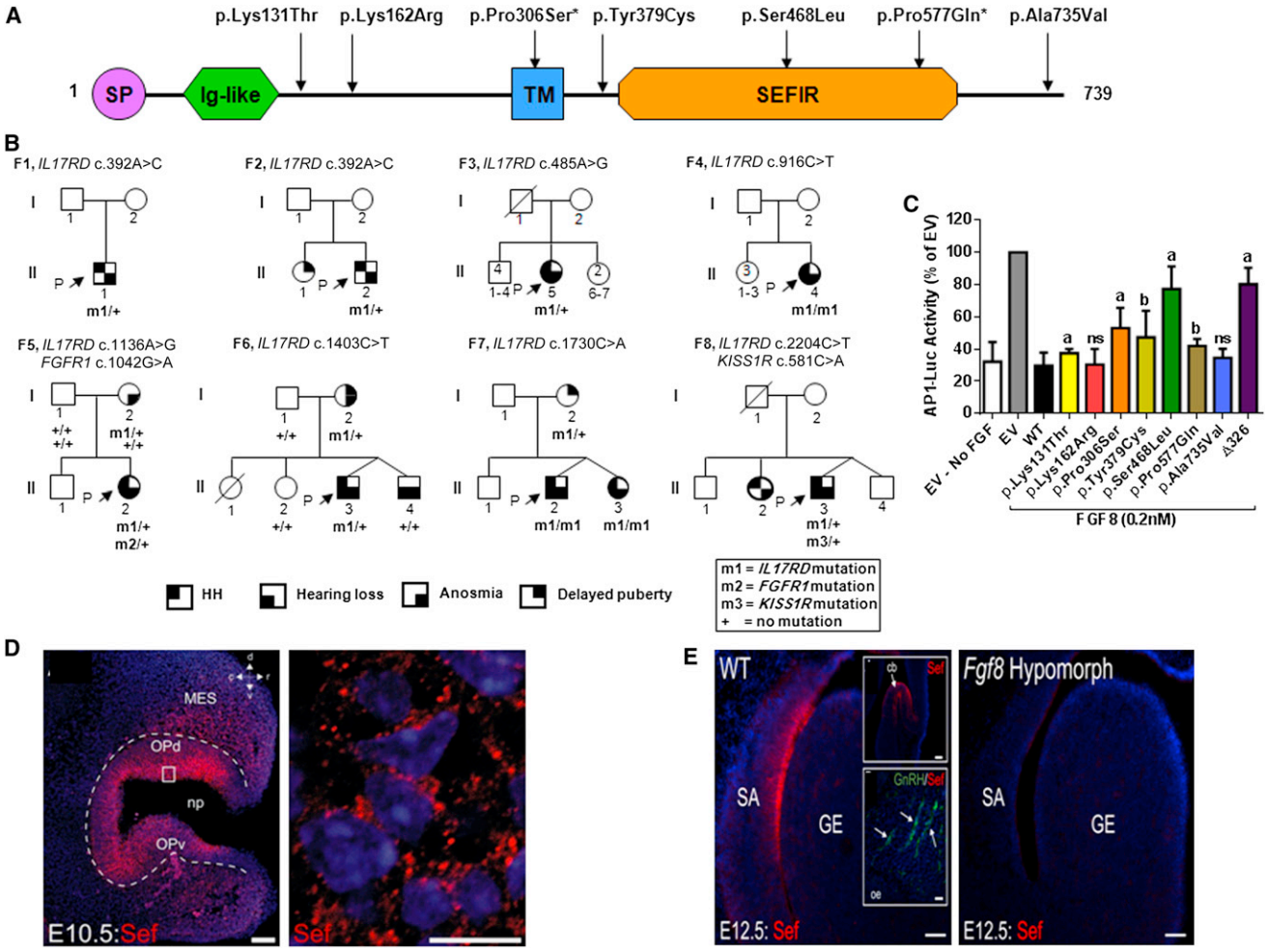

Figure 3. ***IL17RD*** **Mutations in Individuals with CHH**

(A) Schematic of IL17RD domain structure and location of alterations. Abbreviations are as follows: SP, signal peptide; Ig-like, immunoglobulin-like; TM, transmembrane; SEFIR, SEF/IL-17R domain; and *, homozygous.

(B) Pedigrees of KS probands harboring mutations in *IL17RD*. "F" indicates family number. The proband of each family is indicated by an arrow and "P." The available genotypes are indicated below each individual. Numbers within symbols denote the number of additional siblings. Squares depict males, and circles depict females.

(C) Transcription reporter assay of WT and altered IL17RD. HEK293 cells were transiently cotransfected with FGFR1c-encoding cDNA and WT or altered IL17RD together with AP-1 luciferase reporter and then stimulated with FGF8. Plotted are the means ± SEM of five independent experiments run in quadruplet; the results have been normalized to EV-treated cells (100%). The p.Lys131Thr, p.Pro306Ser, and p.Ser468Leu altered proteins showed loss of function in this assay. The p.Tyr379Cys and p.Pro577Gln altered proteins also demonstrated reduced inhibition activity, which was borderline significant ($p = 0.06$). p.Lys162Arg and p.Ala735Val were similar to the WT in this assay. Δ326, a truncated IL17RD lacking the intracellular domain (which is the domain that interacts with FGFR1)[57] served as a negative control. Abbreviations are as follows: a, $p < 0.05$; b, $p = 0.06$; and ns, not significant.

(D) Widefield epifluorescence images of IL17RD immunoreactivity (red) and nuclear marker DAPI (blue) in the nasal region of E10.5 mice (sagittal view) show IL17RD localization in the epithelium of the olfactory placode (left panel). Scale bars represent 100 μm (left panel) and 10 μm (right panel). The area in the white box is enlarged in the right panel. Abbreviations are as follows: MES, mesenchyme; Opd, olfactory placode (dorsal); Opv, olfactory placode (ventral); c, caudal; d, dorsal; r, rostral; and v, ventral; and Sef, similar expression as FGF (former name of IL17RD).

(E) Widefield epifluorescence images of IL17RD immunoreactivity (red) and nuclear marker DAPI (blue) in E12.5 mouse ventral forebrain (sagittal view) of WT (left) and homozygous *Fgf8* hypomorphic (right) embryos illustrate the complete absence of IL17RD in *Fgf8* hypomorphic embryos. IL17RD immunoreactivity was high in the septal area and in the midbrain-hindbrain junction of the WT embryo (upper inset) and nearly undetectable in the olfactory epithelium, where migrating GnRH neurons (green) in the developing nasal regions are localized (lower inset). Scale bars represent 100 μm for all images except the insets, in which they represent 50 μm. Abbreviations are as follows: cb, cerebellum; GE, ganglionic eminence; SA, septal area; and oe, olfactory epithelium; and Sef, similar expression as FGF (former name of IL17RD).

FGFR4 and is specifically contacted by FGF8 subfamily members. Given the homology between FGF17 and FGF8b, we demonstrate that p.Leu342Ser also abolishes FGF17-stimulated signaling through FGFR1c (Figure 4A). These data suggest that FGF17 might be implicated in GnRH neuron biology as an alternative ligand to FGF8b.

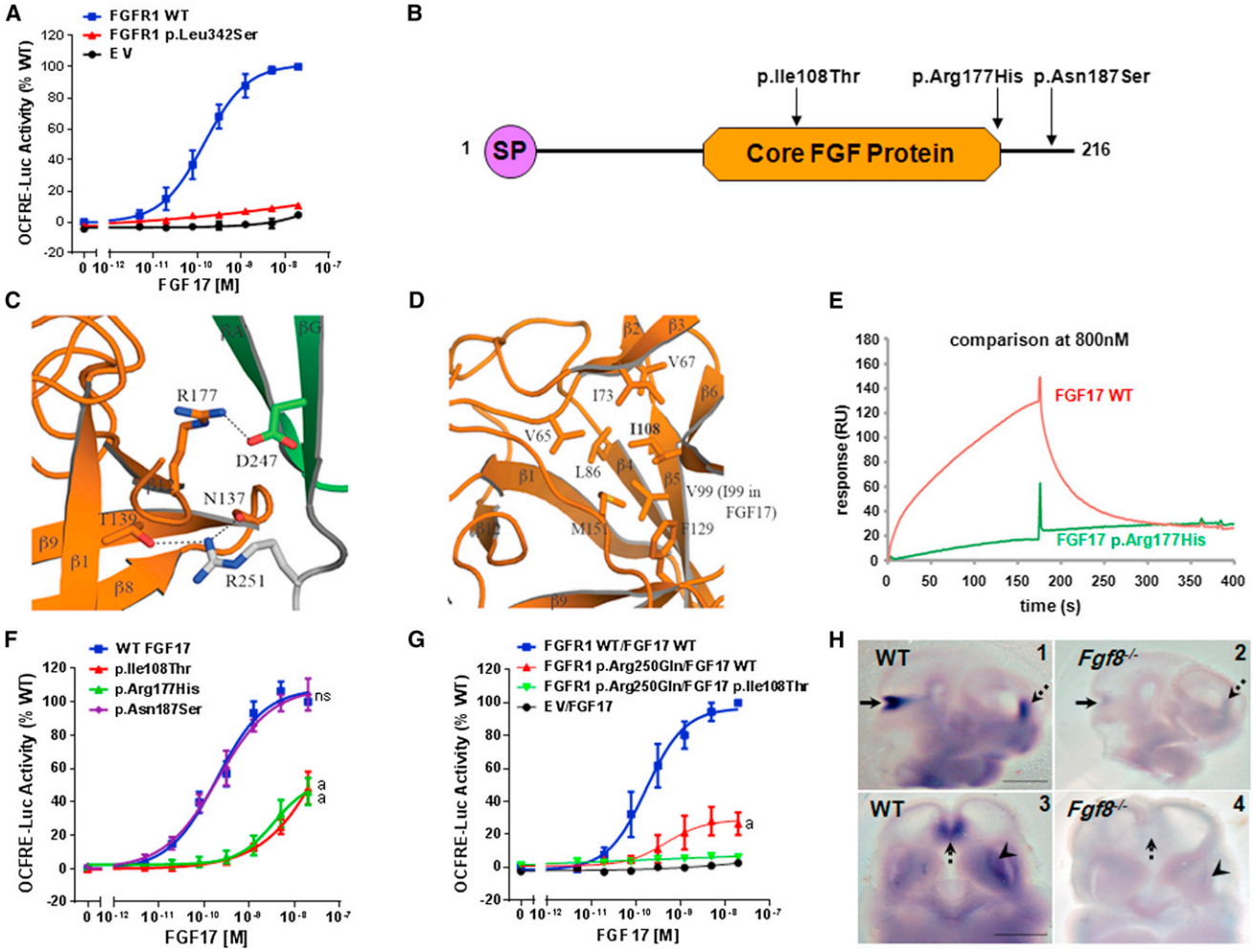

Figure 4. ***FGF17*** **Mutations in Individuals with CHH**

(A) In cells transfected with FGFR1 and a FGF luciferase reporter, increasing doses of WT FGF17 produce a typical sigmoidal dose-response curve (blue), which is abolished by the FGFR1c p.Leu342Ser alteration.

(B) Schematic of FGF17 structural domains and location of the identified alterations. The following abbreviations is used: SP, signal peptide.

(C) The interface between FGF8b (orange) and D2 and D2-D3 linker (green) of FGFR2c as observed in the FGF8b-FGFR2c crystal structure (Protein Data Bank ID 2FDB[37]) depicts the hydrogen bond between Arg177 (R177) of FGF8b and Asp247 (D247) in D2 of FGFR2c and the hydrogen bonds between FGF8b and FGFR Arg251 (R251).

(D) The hydrophobic interior of the β-trefoil core of FGF8b illustrates the hydrophobic interactions among Ile108 (I108), Met151 (M151), Val65 (V65), Val67 (V67), Val99 (V99) (Ile99, I99 in FGF17), Leu86 (L86), Ile73 (I73), and Phe129 (F129).

(E) SPR analysis of the binding of $FGF17^{WT}$ (orange) and $FGF17^{p.Arg177His}$ (green) to the FGFR1c ectodomain. $FGF17^{WT}$ and $FGF17^{p.Arg177His}$ were immobilized onto CM5 sensor chips, and varying concentrations of FGFR1c ectodomain were passed over. The full dose-response curves for $FGF17^{WT}$-FGFR1c and $FGF17^{p.Arg177His}$-FGFR1c binding were generated. For comparison, an overlay of the sensorgrams obtained upon injections of 800 nM solutions of FGFR1c over each ligand is shown.

(F) FGF luciferase-reporter assay showing that the p.Arg177His (green) and p.Ile108Thr (red) FGF17 alterations impair the ligand's biological activity. Abbreviations are as follows: ns, not significant; and a, $p < 0.05$.

(G) The FGFR1c p.Arg250Gln and FGF17 p.Ile108Thr loss-of-function alterations act in additive fashion. Luciferase activity was plotted as the mean ± SEM of three independent experiments performed in triplicate (data are normalized to the WT), and a dose-response curve was fitted as described in Subjects and Methods. The following abbreviation is used: a, $p < 0.05$.

(H) *Fgf17* is expressed in the olfactory placode in a *Fgf8*-dependent manner. *Fgf17* WM-ISH of E10.5 WT (panels 1 and 3) and *Fgf8* homozygous hypomorphic ($Fgf8^{-/-}$; panels 2 and 4) embryos is shown. A 679 nt digoxigenin-labeled *Fgf17* riboprobe was used. Panels 1 and 2 show sagittal views of embryonic heads; scale bars represent 500 mm. Panels 3 and 4 show ventral views of embryonic heads; scale bars represent 250 mm. Arrows are used as follows: solid arrows, midbrain-hindbrain junction; dotted arrows, commissural plate; and arrowheads, medial olfactory placode (where GnRH neurons emerge).

Functional Characterization of the CHH-Associated *FGF17* Mutations

Three unrelated CHH probands harbor heterozygous mutations in *FGF17* (Figures 4B and 5A), and their clinical data are summarized in Table 2. Given the strong sequence identity between FGF8b and FGF17 and their similar receptor-binding-specificity profiles, we employed the previously established FGF8b-FGFR2c structure (Protein Data

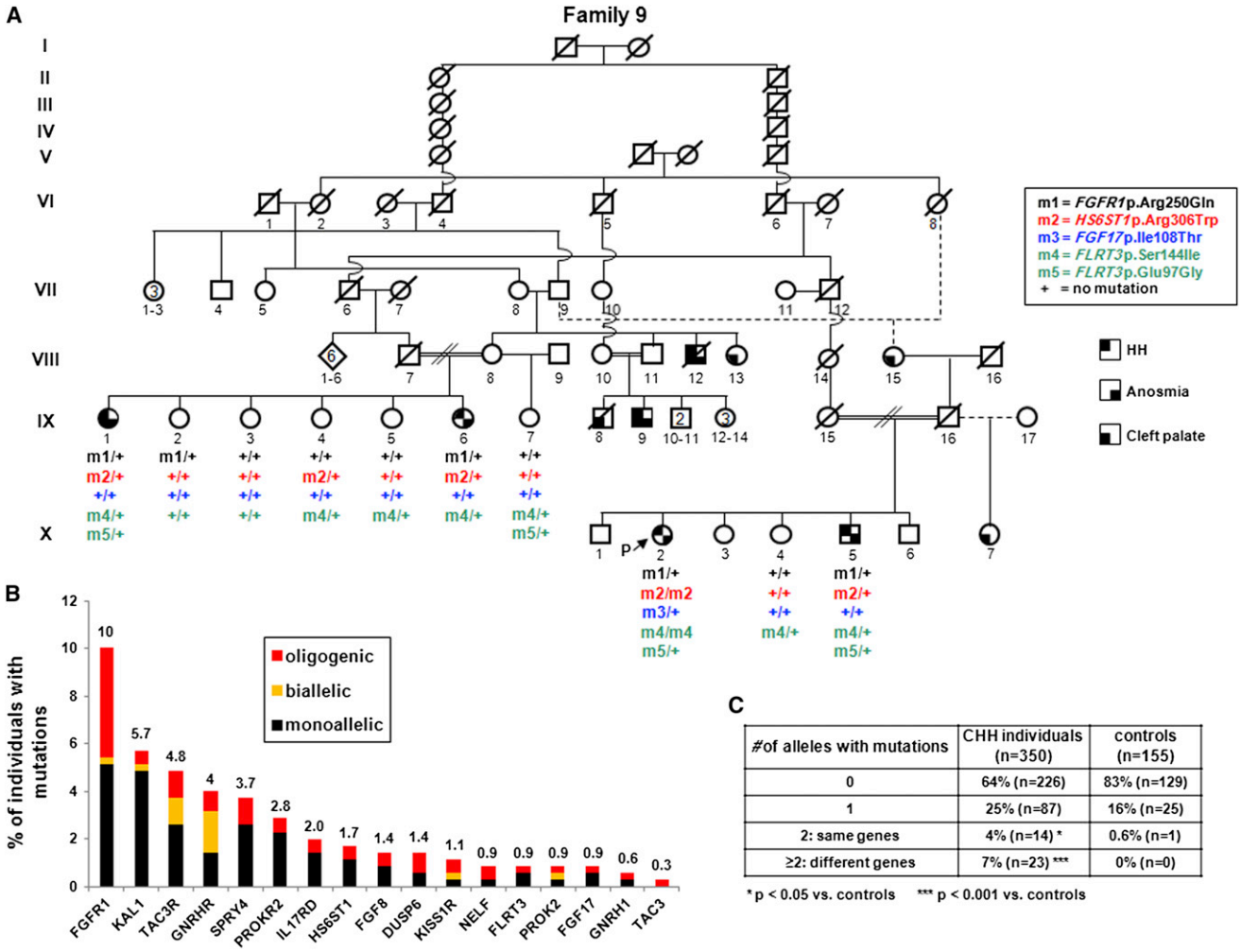

Figure 5. FGF-Network-Associated Genes Contribute to the Oligogenic Architecture of CHH
(A) Pedigree of CHH-affected family with oligogenic inheritance. The proband is indicated by an arrow and "P." The available genotypes are indicated below each individual. Numbers within symbols denote the number of additional siblings. Squares depict males, and circles depict females.
(B) Percentages of individuals with monoallelic, biallelic, and oligogenic mutations in FGF-network-associated genes and/or other genes known to be mutated in CHH.
(C) Number of alleles with mutations in CHH individuals and controls.

Bank ID 2FDB)[37] to model the mutations' impact. FGF17 Arg177 is conserved in FGF8 (Arg177) (Figure S1); in the FGF8b-FGFR2c structure, it forms a hydrogen bond with Asp247 in D2 of FGFR2c. Moreover, the D2 domains of FGFR2c and FGFR1c share strong sequence homology, and FGFR2c Asp247 is conserved in FGFR1c. On the basis of these structural data, it is predicted that the p.Arg177His altered FGF17 cannot form this hydrogen bond and thus has reduced binding to FGFR1c (Figure 4C). FGF17 Ile108 is also conserved in FGF8b (Figure S1), and in the FGF8b-FGFR2c structure, its side chain makes hydrophobic interactions with Met151, Val65, Val67, Val99 (Ile99 in FGF17), Leu86, Ile73, and Phe129 in the hydrophobic interior core. Hence, Ile108 is key for the stability of the β-trefoil core of FGF17 and FGF8. The p.Ile108Thr substitution is predicted to weaken these hydrophobic interactions in the FGF17 core region and to thereby render the mutant ligand less thermally stable and thus prone to unfolding (Figure 4D). The individual harboring the *FGF17* mutation, c.323T>C (p.Ile108Thr), also carries *FGFR1* c.749G>A (p.Arg250Gln), as well as other mutations in genes associated with the FGF8 network (described below). Arg250 is located in the FGFR1c D2-D3 linker region, which is invariably conserved among human FGFRs; Arg250 is pivotal in FGF-FGFR binding affinity through conserved hydrogen bonds with FGF ligands, including FGF8. The p.Arg250Gln substitution is predicted to impair the ability of FGFR1c to bind FGF17. On the other hand, the p.Asn187Ser alteration maps to the C-terminal tail of FGF17 and is predicted to have no impact on FGF17 function.

Consistent with the structural predictions, SPR data showed that the p.Arg177His altered FGF17 exhibited

Table 3. Mutations in 24 Oligogenic Cases among 350 CHH Probands of European Descent

Case	Dx	Sex	Number of Mutations	Number of Mutant Alleles	Gene	Nucleotide Change	Amino Acid Change	Mutation Type	Genotype	MAF in Controls (%)	MAF in CHH Individuals (%)
1	KS	F	4	6	*FGFR1*	c.749G>A	p.Arg250Gln	missense	heterozygous	0	0.4
					FGF17	c.323T>C	p.Ile108Thr	missense	heterozygous	0	0.1
					FLRT3	c.290A>G	p.Glu97Gly	missense	heterozygous	0	0.1
					FLRT3	c.431G>T	p.Ser144Ile	missense	homozygous	0	0.2
					HS6ST1	c.916C>T	p.Arg306Trp	missense	homozygous	0	0.2
2	nIHH	F	3	3	*FGFR1*	c.716T>C	p.Ile239Thr	missense	heterozygous	0	0.1
					PROKR2	c.604A>G	p.Ser202Gly	missense	heterozygous	0	0.1
					GNRH1	c.91C>T	p.Arg31Cys	missense	heterozygous	0	0.1
3	nIHH	F	2	3	*FGFR1*	c.1409G>T	p.Arg470Leu	missense	heterozygous	0	0.1
					GNRHR	c.317A>G	p.Gln106Arg	missense	heterozygous	0.3	1.8
					GNRHR	c.785G>A	p.Arg262Gln	missense	heterozygous	0	0.5
4	nIHH	F	2	3	*FGFR1*	c.350A>G	p.Asn117Ser	missense	heterozygous	0	0.1
					GNRHR	c.247C>G	p.Leu83Val	missense	heterozygous	0	0.1
					GNRHR	c.317A>G	p.Gln106Arg	missense	heterozygous	0.3	1.8
5	nIHH	F	2	3	*FGFR1*	c.2165C>A	p.Pro722His	missense	heterozygous	0	0.1
					FGFR1	c.2172C>G	p.Asn724Lys	missense	heterozygous	0	0.1
					TACR3	c.857A>G	p.Lys286Arg	missense	heterozygous	0.3	0.4
6	nIHH	M	2	3	*FGFR1*	c.2302G>T	p.Asp768Tyr	missense	heterozygous	0	0.1
					FGF8	c.118T>C	p.Phe40Leu	missense	homozygous	0	0.2
7	nIHH	M	2	2	*FGFR1*	c.749G>A	p.Arg250Gln	missense	heterozygous	0	0.4
					FGF8	c.298A>G	p.Lys100Glu	missense	heterozygous	0	0.1
8	nIHH	M	2	2	*FGFR1*	c.1854G>T	p.Lys618Asn	missense	heterozygous	0	0.1
					GNRHR	c.785G>A	p.Arg262Gln	missense	heterozygous	0	0.5
9	nIHH	F	2	2	*FGFR1*	c.682T>G	p.Tyr228Asp	missense	heterozygous	0	0.1
					KISS1R	c.565G>A	p.Ala189Thr	missense	heterozygous	0	0.1
10	KS	M	2	2	*FGFR1*	c.1025T>C	p.Leu342Ser	missense	heterozygous	0	0.1
					NSMF	c.1165-14_22del	-	splice site	heterozygous	0	0.1
11	KS	M	2	2	*FGFR1*	c.1864C>T	p.Arg622*	nonsense	heterozygous	0	0.2
					NSMF	c.587G>A	p.Arg196His	missense	heterozygous	0	0.1
12	KS	M	2	2	*FGFR1*	c.1447C>A	p.Pro483Thr	missense	heterozygous	0	0.1
					SPRY4	c.722C>A	p.Ser241Tyr	missense	heterozygous	0.6	0.5
13	KS	F	2	2	*FGFR1*	c.1042G>A	p.Gly348Arg	missense	heterozygous	0	0.1
					IL17RD	c.1136A>G	p.Tyr379Cys	missense	heterozygous	0	0.1
14	KS	F	2	2	*FGFR1*	c.2008G>A	p.Glu670Lys	missense	heterozygous	0	0.1
					FLRT3	c.205C>A	p.Gln69Lys	missense	heterozygous	0	0.1
15	nIHH	F	2	2	*FGFR1*	c.1553-2A>G	-	splice site	heterozygous	0	0.1
					KAL1	c.1759G>T	p.Val587Leu	missense	heterozygous	0.4	0.2
16	KS	M	2	2	*FGFR1*	c.2075A>G	p.Glu692Gly	missense	heterozygous	0	0.1
					DUSP6	c. 545C>T	p.Ser182Phe	missense	heterozygous	0	0.1

(*Continued on next page*)

Table 3. *Continued*

Case	Dx	Sex	Number of Mutations	Number of Mutant Alleles	Gene	Nucleotide Change	Amino Acid Change	Mutation Type	Genotype	MAF in Controls (%)	MAF in CHH Individuals (%)
17	KS	F	2	2	*FGFR1*	c.1755C>A	p.Tyr585*	nonsense	heterozygous	0	0.1
					TACR3	c.1091G>A	p.Arg364Gln	missense	heterozygous	0	0.1
18	KS	F	2	2	*DUSP6*	c.566A>G	p.Asn189Ser	missense	heterozygous	0	0.2
					SPRY4	c.722C>A	p.Ser241Tyr	missense	heterozygous	0.6	0.5
19	KS	F	2	2	*DUSP6*	c.1037C>T	p.Thr346Met	missense	heterozygous	0	0.1
					SPRY4	c.722C>A	p.Ser241Tyr	missense	heterozygous	0.6	0.5
20	nIHH	F	2	2	*SPRY4*	c.722C>A	p.Ser241Tyr	missense	heterozygous	0.6	0.5
					TACR3	c.1345G>A	p.Ala449Thr	missense	heterozygous	0.6	0.5
21	KS	M	2	2	*IL17RD*	c.2204C>T	p.Ala735Val	missense	heterozygous	0	0.1
					KISS1R	c.581C>A	p.Ala194Asp	missense	heterozygous	0	0.1
22	nIHH	F	2	2	*HS6ST1*	c.1144C>T	p.Arg382Trp	missense	heterozygous	0	0.2
					TAC3	c.238C>A	p.Arg80Ser	missense	heterozygous	0	0.1
23	KS	M	2	2	*KAL1*	c.571C>T	p.Arg191*	nonsense	hemizygous	0	0.2
					TACR3	c.1345G>A	p.Ala449Thr	missense	heterozygous	0.6	0.5
24	KS	F	2	2	*PROK2*	c.70G>C	p.Ala24Pro	missense	heterozygous	0	0.1
					PROKR2	c.343G>A	p.Val115Met	missense	heterozygous	0	0.1

Abbreviations are as follows: F, female; and M, male.

negligible binding to FGFR1c (Figure 4E). Moreover, the p.Arg177His altered FGF17 had dramatically reduced ability to activate FGFR1c (Figure 4F); the p.Ile108Thr altered FGF17 was also defective in FGFR1c activation, whereas the p.Asn187Ser altered FGF17 was indistinguishable from the WT (Figure 4F). Finally, the p.Arg250Gln altered FGFR1c caused severe loss of function (Figure 4G). Because the *FGFR1c* c.749G>A (p.Arg250Gln) and *FGF17* c.323T>C (p.Ile108Thr) mutations co-occur in the same individual, we exposed cells expressing the altered receptor to the altered ligand; relative to WT FGF17, the p.Ile108Thr FGF17 completely failed to activate the p.Arg250Gln FGFR1c, indicating that these two loss-of-function substitutions act in an additive fashion (Figure 4G).

FGF8 Is Required for *Fgf17* Expression in the Olfactory Placode

To link *Fgf17* to GnRH biology, we examined its expression pattern in the nasal cavity of mouse embryos through WM-ISH at E10.5, when GnRH neuron fate specification occurs. *Fgf17* was robustly expressed in regions where *Fgf8* is known to be highly expressed: the commissural plate (Figures 4H1 and 4H3), the midbrain-hindbrain junction (Figure 4H1), and the medial olfactory placode (Figure 4H3), where GnRH neurons emerge.[19] Importantly, there was hardly any *Fgf17* expression in *Fgf8* hypomorphic mice (Figures 4H2 and 4H4), suggesting that *Fgf17* should be considered a member of the *Fgf8* synexpression group.

Mutations in FGF8-Network-Associated Genes Contribute to Oligogenic CHH

To assess oligogenicity, we investigated a subset of individuals comprising all European-descendent probands (n = 350/386) and controls (n = 155/155) screened for the nine genes associated with the FGF pathway. Seventeen genes were analyzed (the nine genes encoding members of the FGF network [Figure 1A] and eight others: *PROKR2*, *PROK2*, *KISS1R*, *GNRHR*, *GNRH1*, *TAC3R*, *TAC3*, and *NSMF*). We identified mutations in 35% of probands (124/350) (Table S3). Nearly all mutations in the 17 genes cause loss of function in vitro and/or are predicted in silico to be deleterious (Table S1).[39–41,59–62] Notably, 69% (86/124) of these CHH probands harbor at least one mutation within the genes encoding members of the FGF network (Table S3), highlighting the major contribution of mutations affecting this pathway to the genetic architecture of CHH. Of the 124 probands harboring mutations, 14 carry biallelic mutations in the same gene (i.e., 11% homozygosity or compound heterozygosity) and 24 carry at least two mutant alleles from different genes (i.e., 19% oligogenicity; 95% confidence interval: 12%–26%) (Figures 5B and 5C and Tables 3 and S3). In 23/24 cases, the oligogenic interactions include at least one gene associated with the FGF network (Figure 5B and Table 3). Among the controls, 16% (25/155) harbor missense mutations; each subject carries a single heterozygous mutation (Table S4). Four mutations (with MAF < 1% in controls) within genes encoding components of the FGF network are also present in the CHH

cohort (Table S4): *FGF8* c.77C>T (p.Pro26Leu), *IL17RD* c.392A>C (p.Lys131Thr), *KAL1* c.1759G>T (p.Val587Leu), and *SPRY4* c.722C>A (p.Ser241Tyr) (Table S4). Notably, most CHH probands harboring a mutation present in the control population also carry an additional gene defect. This is consistent with the fact that oligogenicity was found only in probands and never in controls (24/350 versus 0/155, $p = 0.0003$; Figure 5C); biallelic mutations (homozygous or compound heterozygous) were also more frequent in probands than in controls (14/350 versus 1/155, $p = 0.04$; Figure 5C).

The female KS individual (Table 3, case 1) is a notable example of oligogenicity: she not only carries the *FGF17* c.323T>C (p.Ile108Thr) loss-of-function mutation but also harbors previously characterized mutations in *FGFR1* (c.749G>A [p.Arg250Gln]; heterozygous) and *HS6ST1* (c.916C>T [p.Arg360Trp]; homozygous),[15] as well as mutations in *FLRT3*, c.431G>T (p.Ser144Ile) (homozygous) and c.290A>G (p.Glu96Gly) (heterozygous) (Figure 5A, X-2 in family 9). She had primary amenorrhea (successfully treated with pulsatile GnRH, resulting in ovulation), severe osteoporosis (Z score $= -3$) with multiple fractures, surgery for bilateral genu valgus, and severe obesity and developed type 2 diabetes before 40 years of age. The proband is part of a large French Canadian family (previously described in great detail) with several loops of consanguinity and in which 27% of family members exhibit CHH.[63] Interestingly, our genetic analysis revealed that all affected subjects in this pedigree harbor a loss-of-function *FGFR1* c.749G>A (p.Arg250Gln) mutation, as well as other mutations in genes associated with the FGF network: each affected CHH family member (IX-1, IX-6, X-2, and X-5 in family 9) carries three to six mutant alleles among four different FGF-network-associated genes (*FGF17*, *FLRT3*, *HS6ST1*, and *FGFR1*), whereas asymptomatic family members (IX-2, IX-3, IX-4, IX-5, IX-7, and X-4 in family 9) harbor zero to two mutant alleles. In another notable case of oligogenicity, the KS proband (Figure 3B, F5 II-2) harbors a loss-of-function heterozygous c.1136A>G (p.Tyr379Cys) *IL17RD* mutation inherited from her anosmic mother (I-2 in F5). However, the female proband also harbors a de novo heterozygous c.1042G>A (p.Gly348Arg) *FGFR1* mutation that is predicted to cause loss of function by all four in silico prediction programs (Table S1). This combination manifested in the proband with a severe phenotype including KS with dental agenesis, hearing loss, osteoporosis, and a complete absence of puberty.

Discussion

In this work, we identify mutations in five genes encoding components of the FGF pathway (*FGF17*, *IL17RD*, *SPRY4*, *DUSP6*, and *FLRT3*) in CHH individuals. All together, 27 mutations were found in 30 unrelated CHH probands, and mutations in each gene accounted for 1%–4% of CHH cases. Together with the other FGF-network-associated genes previously known to be mutated in CHH (*FGFR1*, *FGF8*, *KAL1*, and *HS6ST1*), 23% (90/386) of CHH individuals have at least one mutation affecting the FGF pathway, indicating a major contribution of this network to GnRH ontogeny. The majority of probands display olfactory defects, consistent with the critical role of the FGF8 synexpression group in early stages of GnRH neuron development. Traditionally, the average success rate of candidate-gene approaches in CHH is ~30%;[3] 70% of the screened candidate genes associated with the expanded FGF network had mutations. There were two orthogonal components to the successful strategy: (1) focus on the "FGF8 synexpression group" and (2) utilization of a bioinformatics algorithm for gene prediction and prioritization.

Genes that are "synexpressed" with *FGF8* share a similar spatiotemporal expression with *FGF8* during development, and the proteins they encode specifically modulate the efficiency of FGF8 signaling through FGFR1c (Figure 1A).[16–18] Alterations in the modulators (inhibitors or activators) of FGF8 most likely disrupt the fine-tuning of FGF8 signaling, leading to abnormal development of GnRH neurons and the olfactory system. The mechanisms by which altered FGF8 signaling impacts GnRH neuron fate specification are not well understood, largely because no marker for GnRH neuron progenitors is known. Still, it is known that FGF8 is a potent cell-survival factor during early neural development in the forebrain and the midbrain-hindbrain boundary, as well as for migrating neural crest and olfactory stem cells.[64] Consistently, *Fgf8*-conditional-knockout mice exhibit increased levels of apoptosis in the developing olfactory epithelium (OE) between E10.5 and E12.5;[65] thus, decreased FGF8 signaling might lead to premature elimination of GnRH progenitor cells. Recently, FGF8 was shown to maintain the gene-expression signatures and proliferative identities of two precursor classes in the OE: MEIS-positive cells (which reside in the lateral OE) and SOX2- and ASCL1-positive cells (which reside in the medial OE). Thus, decreased FGF8 signaling might hamper progenitor cells from becoming GnRH neurons.[66]

The second component to the strategy applied was an unbiased approach to identifying high-quality candidate genes by analyzing the interactome of proteins encoded by genes known to be mutated in CHH independently of the synexpression data. Among the entire proteome, the IBAS algorithm awarded significant scores to a small set of 36 proteins, among which IL17RD and FGF17 were the top ranked. Although one might intuitively expect that proteins related to FGFR1-FGF8 signaling would score well in IBAS, such results were not observed for other receptor-ligand pairs associated with CHH. In fact, the FGF8-associated proteins were awarded high scores because they have been shown to have high-quality, specific interactions with FGFR1 and/or FGF8. Because FGFR1 has >300 annotated interaction partners in InWeb, it was not itself awarded a significant IBAS score because the likelihood of interacting directly with 1/14

CHH-associated proteins (in this case, FGF8) given a total of 300 annotated interaction partners is not significant. Thus, the identification by IBAS of IL17RD and FGF17 as the top two candidates, matching the results of the genetic analysis, indicates that IBAS is a powerful methodology for genome-scale candidate prioritization. IBAS, along with many more details, will be made broadly available as a community resource (K. Lage, unpublished data).

The top protein prioritized by IBAS (IL17RD) was validated by the identification of homozygous and heterozygous mutations in KS probands. IL17RD is a single transmembrane glycoprotein with sequence similarity to the intracellular domain of the interleukin-17 receptor; it is one of the major antagonists of FGF downstream signaling in vivo[16,18] and in vitro.[57,58] The mechanisms by which IL17RD inhibits FGF signaling are contentious because it has been shown to act both at the level of the FGF receptors (FGFR1 and FGFR2)[18] and on downstream components of the Ras-ERK1/2 pathway by capturing active MEK and ERK complexes at the Golgi apparatus and inhibiting their dissociation.[16,58] Close spatiotemporal interdependence between FGF signaling and IL17RD expression has been reported in various mammalian tissues.[67] Here, we document high IL17RD expression in the olfactory epithelium at E10.5, coinciding with the timeframe of GnRH neuronal fate specification, which is dependent on FGF8. The coexpression of IL17RD with FGF8 in the olfactory placode during embryogenesis suggests a potential role in the early development of both GnRH and olfactory neurons. Notably, most of the *IL17RD* mutations identified were shown to cause loss of function; given that IL17RD is an inhibitor, the mutations increase FGF8 signaling in vitro. This might appear counterintuitive given that CHH-associated loss-of-function mutations in *FGF8*, *FGFR1*, *KAL1*, and *HS6ST1* described thus far lead to decreased FGF8 signaling. Nevertheless, *Il17rd*$^{-/-}$ mice (which display increased FGF8 activity) and *IL17RD*-overexpressing chickens (which display decreased FGF8 activity) both show defects in the cochlear nucleus and dysfunction of the auditory brainstem.[25] Moreover, complete elimination or overexpression of FGF8 increased apoptosis in olfactory progenitor cells, whereas a lesser decrease in functional FGF8 expression resulted in cell survival, suggesting nonlinear dosage effects.[68]

All studied individuals with *IL17RD* mutations have KS, and the fact that six out of eight (75%) have hearing loss suggests a frequency much higher than the 6% reported previously.[69] It appears that either biallelic *IL17RD* mutations or an additional mutation in another locus is needed to cause KS or hearing loss. The hearing-loss phenotype is consistent with the fact that IL17RD is a powerful inhibitor of FGF8 signaling: acting through FGFR1c, FGF8 is a morphogen for otic development in both chickens and mice.[7,70] In zebrafish, the injection of *sef* (also called *il17rd*) mRNA into embryos produces a phenotype similar to that of *fgf8* deficiency, including a smaller otic vesicle.[16] Further, *Il17rd*$^{-/-}$ mice or *IL17RD*-overexpressing chickens exhibit auditory brainstem defects.[25] Thus, IL17RD appears to be critical not only for GnRH neuron ontogeny but also for the normal development of the auditory system by modulating FGF signaling. The present study was not specifically designed to investigate the frequency of *IL17RD* mutations among CHH individuals with hearing loss; after the identification of *IL17RD* as a locus for CHH with this particular subphenotype, a next logical step is to screen a larger cohort of CHH individuals with hearing loss for mutations in *IL17RD*. Moreover, because CHH is usually only diagnosed at or after the age of puberty, it would be interesting to test prepubertal individuals with congenital hearing loss for this gene, especially those with other clinical manifestations suggestive of KS (i.e., cryptorchidism, anosmia, skeletal defects, etc.).

The second-highest ranked gene was *FGF17*, which emerged as the gene encoding the second-most critical FGFR1c ligand for GnRH neuron ontogeny. This link is based on (1) the decreased binding of FGF17 to the KS-associated c.1025T>C (p.Leu342Ser) *FGFR1c* mutant, (2) the identification of loss-of-function *FGF17* mutations in CHH individuals with severe associated skeletal anomalies, and (3) the demonstration that *Fgf17* is a member of the *Fgf8* synexpression group in the medial aspect of the olfactory placode in E10.5 mice, where its expression requires *Fgf8*. Mice lacking FGF17 have cerebellar defects and selective reduction in the size of the dorsal frontal cortex, consistent with a role similar to that of FGF8 in patterning the neocortical map. However, the olfactory bulbs seem unaffected in FGF17-deficient mice; thus, FGF17 appears to be a less powerful morphogen than FGF8.[20] Similarly to that of other FGF subfamilies, the expansion of the FGF8 group has most likely been contributed to by gene-duplication events throughout evolution. The high conservation of FGF17 suggests that, in addition to providing functional redundancy with FGF8, it might have evolved unique roles for each subfamily member. In this regard, it is interesting that in adult zebrafish, Fgf8 signaling is restricted to the periventricular area whereas Fgf17 is widely expressed in the hypothalamus[21] because this suggests a different function for Fgf17, such as a potential role in GnRH neuron survival in adulthood.

The mutations in *DUSP6*, *SPRY4*, and *FLRT3* were not functionally characterized in this study. These members of the *FGF8* synexpression module play pleitropic roles in embryogenesis and adulthood. DUSP6 is a dual-specificity protein phosphatase, which dephosphorylates and thereby inactivates MAP kinases.[32] In rat PC12 cells, DUSP6 reduces neurotransmitter release by decreasing the expression of the L-type calcium channel cav1.2.[71] In mice, a *Dusp6* mutant allele causes variably penetrant, dominant postnatal lethality, skeletal dwarfism, premature fusion of the cranial sutures (craniosynostosis), and hearing loss.[32] SPRY proteins antagonize FGF signaling by inhibiting the receptor-induced activation of the MAPK pathway; SPRYs are positioned upstream of RAS activation and impair the formation of active GTP-RAS.[72] SPRY4

regulates neurite outgrowth in rat PC12 cells and mouse hippocampal neurons in culture by inhibiting the MAPK pathway;[73,74] *Spry4*$^{-/-}$ mice have craniofacial defects and abnormal limb development.[29] *FLRT3* encodes a transmembrane cell-adhesion protein that is characterized by a cluster of leucine-rich repeats and one fibronectin type III domain within its extracellular region. Its action promotes the activation of FGF signaling by increasing ERK phosphorylation.[34] FLRT3 positively regulates neurite outgrowth in rat neuronal cells[36] and acts as a repulsive guidance cue for UNC5-positive neurons in mice.[75] The present identification of mutations in *DUSP6*, *SPRY4*, and *FLRT3* in CHH individuals might offer new opportunities for studies of these genes in GnRH biology.

Studying *FGFR1* mutations in CHH has been pivotal in challenging the traditional monogenic view of this disorder and in transitioning toward more complex genetic models.[5,39,53] Proof of concept for the oligogenic paradigm has been provided by model organisms; for example, *Fgfr1*$^{+/-}$ *Fgf8*$^{+/-}$ double heterozygous mice show an additive loss of GnRH neurons,[76] and Il17rd and Spry2 synergize in zebrafish to regulate the expression of Gbx2 in the mid-hindbrain region.[77] The present identification of five additional genes with mutations in CHH expands not only the percentage of cases with a known genetic cause but also the percentage of individuals with evidence of oligogenicity: among the 17 genes analyzed, oligogenicity accounts for 19% of individuals compared to 10% in prior work examining eight CHH loci.[39] The updated frequency of oligogenicity (19%) considers only the one-third of individuals (124/350) found to harbor at least one mutation; we therefore anticipate that the true frequency of oligogenicity in CHH is substantially higher and that our estimates will better approach it as mutations are identified in further loci, especially through application of next-generation-sequencing technologies to large CHH cohorts.

Supplemental Data

Supplemental Data include two figures and five tables and can be found with this article online at http://www.cell.com/AJHG.

Acknowledgments

We thank the individuals and their families for their invaluable and enthusiastic participation. This work was supported by the Eunice Kennedy Shriver National Institute of Child Health and Human Development/National Institutes of Health R01HD056264 (N.P.), R01HD15788 (W.C.), through Cooperative Agreement U54HD028138 as part of the Specialized Cooperative Centers Program in Reproduction and Infertility Research, 2R01DE013686-11 (MM), NINDS R01 NS34661 (J.R.), the Swiss National Science Foundation (N.P.), and COST Action BM1105.

Received: December 31, 2012
Revised: March 14, 2013
Accepted: April 10, 2013
Published: May 2, 2013

Web Resources

The URLs for data presented herein are as follows:

1000 Genomes, http://browser.1000genomes.org
Allen Mouse Brain Atlas, http://mouse.brain-map.org
Berkeley Drosophila Genome Project (BDGP) Splice Site Prediction by Neural Network, http://www.fruitfly.org/seq_tools/splice.html
Brain Gene Expression Map, http://www.stjudebgem.org/web/mainPage/mainPage.php
dbSNP, http://www.ncbi.nlm.nih.gov/projects/SNP
Ensembl Genome Browser, http://www.ensembl.org/index.html
Human Genome Variation Society, http://www.hgvs.org/mutnomen/
InWeb, http://www.cbs.dtu.dk/suppl/dgf/heart_developmental_networks/index.php
Mouse Genome Informatics, http://www.informatics.jax.org/
MutationTaster, http://www.mutationtaster.org/
NCBI Genome Browser, http://www.ncbi.nlm.nih.gov/sites/entrez?db=Genome
NHLBI Exome Sequencing Project (ESP) Exome Variant Server, http://evs.gs.washington.edu/EVS/
Online Mendelian Inheritance in Man (OMIM), http://www.omim.org/
PMut, http://mmb.pcb.ub.es/PMut/
PolyPhen-2, www.genetics.bwh.harvard.edu/pph2/
RefSeq, http://www.ncbi.nlm.nih.gov/RefSeq
SIFT, http://sift.jcvi.org/
UCSC Genome Browser, http://genome.ucsc.edu
UniProt, http://www.uniprot.org/

References

1. Bianco, S.D., and Kaiser, U.B. (2009). The genetic and molecular basis of idiopathic hypogonadotropic hypogonadism. Nat. Rev. Endocrinol. *5*, 569–576.
2. Quinton, R., Duke, V.M., Robertson, A., Kirk, J.M., Matfin, G., de Zoysa, P.A., Azcona, C., MacColl, G.S., Jacobs, H.S., Conway, G.S., et al. (2001). Idiopathic gonadotrophin deficiency: genetic questions addressed through phenotypic characterization. Clin. Endocrinol. (Oxf.) *55*, 163–174.
3. Sykiotis, G.P., Pitteloud, N., Seminara, S.B., Kaiser, U.B., and Crowley, W.F., Jr. (2010). Deciphering genetic disease in the genomic era: the model of GnRH deficiency. Sci. Transl. Med. *2*, rv2.
4. Dodé, C., Levilliers, J., Dupont, J.M., De Paepe, A., Le Dû, N., Soussi-Yanicostas, N., Coimbra, R.S., Delmaghani, S., Compain-Nouaille, S., Baverel, F., et al. (2003). Loss-of-function mutations in FGFR1 cause autosomal dominant Kallmann syndrome. Nat. Genet. *33*, 463–465.
5. Falardeau, J., Chung, W.C., Beenken, A., Raivio, T., Plummer, L., Sidis, Y., Jacobson-Dickman, E.E., Eliseenkova, A.V., Ma, J., Dwyer, A., et al. (2008). Decreased FGF8 signaling causes deficiency of gonadotropin-releasing hormone in humans and mice. J. Clin. Invest. *118*, 2822–2831.
6. Chung, W.C., Moyle, S.S., and Tsai, P.S. (2008). Fibroblast growth factor 8 signaling through fibroblast growth factor receptor 1 is required for the emergence of gonadotropin-releasing hormone neurons. Endocrinology *149*, 4997–5003.
7. Ladher, R.K., Wright, T.J., Moon, A.M., Mansour, S.L., and Schoenwolf, G.C. (2005). FGF8 initiates inner ear induction in chick and mouse. Genes Dev. *19*, 603–613.

8. Martinez-Morales, J.R., Del Bene, F., Nica, G., Hammerschmidt, M., Bovolenta, P., and Wittbrodt, J. (2005). Differentiation of the vertebrate retina is coordinated by an FGF signaling center. Dev. Cell *8*, 565–574.
9. Perantoni, A.O., Timofeeva, O., Naillat, F., Richman, C., Pajni-Underwood, S., Wilson, C., Vainio, S., Dove, L.F., and Lewandoski, M. (2005). Inactivation of FGF8 in early mesoderm reveals an essential role in kidney development. Development *132*, 3859–3871.
10. Lewandoski, M., Sun, X., and Martin, G.R. (2000). Fgf8 signalling from the AER is essential for normal limb development. Nat. Genet. *26*, 460–463.
11. Miraoui, H., Dwyer, A., and Pitteloud, N. (2011). Role of fibroblast growth factor (FGF) signaling in the neuroendocrine control of human reproduction. Mol. Cell. Endocrinol. *346*, 37–43.
12. Franco, B., Guioli, S., Pragliola, A., Incerti, B., Bardoni, B., Tonlorenzi, R., Carrozzo, R., Maestrini, E., Pieretti, M., Taillon-Miller, P., et al. (1991). A gene deleted in Kallmann's syndrome shares homology with neural cell adhesion and axonal path-finding molecules. Nature *353*, 529–536.
13. Legouis, R., Hardelin, J.P., Levilliers, J., Claverie, J.M., Compain, S., Wunderle, V., Millasseau, P., Le Paslier, D., Cohen, D., Caterina, D., et al. (1991). The candidate gene for the X-linked Kallmann syndrome encodes a protein related to adhesion molecules. Cell *67*, 423–435.
14. González-Martínez, D., Kim, S.H., Hu, Y., Guimond, S., Schofield, J., Winyard, P., Vannelli, G.B., Turnbull, J., and Bouloux, P.M. (2004). Anosmin-1 modulates fibroblast growth factor receptor 1 signaling in human gonadotropin-releasing hormone olfactory neuroblasts through a heparan sulfate-dependent mechanism. J. Neurosci. *24*, 10384–10392.
15. Tornberg, J., Sykiotis, G.P., Keefe, K., Plummer, L., Hoang, X., Hall, J.E., Quinton, R., Seminara, S.B., Hughes, V., Van Vliet, G., et al. (2011). Heparan sulfate 6-O-sulfotransferase 1, a gene involved in extracellular sugar modifications, is mutated in patients with idiopathic hypogonadotrophic hypogonadism. Proc. Natl. Acad. Sci. USA *108*, 11524–11529.
16. Fürthauer, M., Lin, W., Ang, S.L., Thisse, B., and Thisse, C. (2002). Sef is a feedback-induced antagonist of Ras/MAPK-mediated FGF signalling. Nat. Cell Biol. *4*, 170–174.
17. Niehrs, C., and Meinhardt, H. (2002). Modular feedback. Nature *417*, 35–36.
18. Tsang, M., Friesel, R., Kudoh, T., and Dawid, I.B. (2002). Identification of Sef, a novel modulator of FGF signalling. Nat. Cell Biol. *4*, 165–169.
19. Bachler, M., and Neubüser, A. (2001). Expression of members of the Fgf family and their receptors during midfacial development. Mech. Dev. *100*, 313–316.
20. Cholfin, J.A., and Rubenstein, J.L. (2007). Patterning of frontal cortex subdivisions by Fgf17. Proc. Natl. Acad. Sci. USA *104*, 7652–7657.
21. Topp, S., Stigloher, C., Komisarczuk, A.Z., Adolf, B., Becker, T.S., and Bally-Cuif, L. (2008). Fgf signaling in the zebrafish adult brain: association of Fgf activity with ventricular zones but not cell proliferation. J. Comp. Neurol. *510*, 422–439.
22. Xu, J., Liu, Z., and Ornitz, D.M. (2000). Temporal and spatial gradients of Fgf8 and Fgf17 regulate proliferation and differentiation of midline cerebellar structures. Development *127*, 1833–1843.
23. Liu, Z., Xu, J., Colvin, J.S., and Ornitz, D.M. (2002). Coordination of chondrogenesis and osteogenesis by fibroblast growth factor 18. Genes Dev. *16*, 859–869.
24. Ohbayashi, N., Shibayama, M., Kurotaki, Y., Imanishi, M., Fujimori, T., Itoh, N., and Takada, S. (2002). FGF18 is required for normal cell proliferation and differentiation during osteogenesis and chondrogenesis. Genes Dev. *16*, 870–879.
25. Abraira, V.E., Hyun, N., Tucker, A.F., Coling, D.E., Brown, M.C., Lu, C., Hoffman, G.R., and Goodrich, L.V. (2007). Changes in Sef levels influence auditory brainstem development and function. J. Neurosci. *27*, 4273–4282.
26. Mailleux, A.A., Tefft, D., Ndiaye, D., Itoh, N., Thiery, J.P., Warburton, D., and Bellusci, S. (2001). Evidence that SPROUTY2 functions as an inhibitor of mouse embryonic lung growth and morphogenesis. Mech. Dev. *102*, 81–94.
27. de Maximy, A.A., Nakatake, Y., Moncada, S., Itoh, N., Thiery, J.P., and Bellusci, S. (1999). Cloning and expression pattern of a mouse homologue of drosophila sprouty in the mouse embryo. Mech. Dev. *81*, 213–216.
28. Shim, K., Minowada, G., Coling, D.E., and Martin, G.R. (2005). Sprouty2, a mouse deafness gene, regulates cell fate decisions in the auditory sensory epithelium by antagonizing FGF signaling. Dev. Cell *8*, 553–564.
29. Taniguchi, K., Ayada, T., Ichiyama, K., Kohno, R., Yonemitsu, Y., Minami, Y., Kikuchi, A., Maehara, Y., and Yoshimura, A. (2007). Sprouty2 and Sprouty4 are essential for embryonic morphogenesis and regulation of FGF signaling. Biochem. Biophys. Res. Commun. *352*, 896–902.
30. Leeksma, O.C., Van Achterberg, T.A., Tsumura, Y., Toshima, J., Eldering, E., Kroes, W.G., Mellink, C., Spaargaren, M., Mizuno, K., Pannekoek, H., and de Vries, C.J. (2002). Human sprouty 4, a new ras antagonist on 5q31, interacts with the dual specificity kinase TESK1. Eur. J. Biochem. *269*, 2546–2556.
31. Dickinson, R.J., Eblaghie, M.C., Keyse, S.M., and Morriss-Kay, G.M. (2002). Expression of the ERK-specific MAP kinase phosphatase PYST1/MKP3 in mouse embryos during morphogenesis and early organogenesis. Mech. Dev. *113*, 193–196.
32. Li, C., Scott, D.A., Hatch, E., Tian, X., and Mansour, S.L. (2007). Dusp6 (Mkp3) is a negative feedback regulator of FGF-stimulated ERK signaling during mouse development. Development *134*, 167–176.
33. Vieira, C., and Martinez, S. (2005). Experimental study of MAP kinase phosphatase-3 (Mkp3) expression in the chick neural tube in relation to Fgf8 activity. Brain Res. Brain Res. Rev. *49*, 158–166.
34. Böttcher, R.T., Pollet, N., Delius, H., and Niehrs, C. (2004). The transmembrane protein XFLRT3 forms a complex with FGF receptors and promotes FGF signalling. Nat. Cell Biol. *6*, 38–44.
35. Maretto, S., Müller, P.S., Aricescu, A.R., Cho, K.W., Bikoff, E.K., and Robertson, E.J. (2008). Ventral closure, headfold fusion and definitive endoderm migration defects in mouse embryos lacking the fibronectin leucine-rich transmembrane protein FLRT3. Dev. Biol. *318*, 184–193.
36. Robinson, M., Parsons Perez, M.C., Tébar, L., Palmer, J., Patel, A., Marks, D., Sheasby, A., De Felipe, C., Coffin, R., Livesey, F.J., and Hunt, S.P. (2004). FLRT3 is expressed in sensory neurons after peripheral nerve injury and regulates neurite outgrowth. Mol. Cell. Neurosci. *27*, 202–214.
37. Olsen, S.K., Li, J.Y., Bromleigh, C., Eliseenkova, A.V., Ibrahimi, O.A., Lao, Z., Zhang, F., Linhardt, R.J., Joyner, A.L., and Mohammadi, M. (2006). Structural basis by which alternative splicing modulates the organizer activity of FGF8 in the brain. Genes Dev. *20*, 185–198.
38. Pitteloud, N., Hayes, F.J., Dwyer, A., Boepple, P.A., Lee, H., and Crowley, W.F., Jr. (2002). Predictors of outcome of long-term

GnRH therapy in men with idiopathic hypogonadotropic hypogonadism. J. Clin. Endocrinol. Metab. *87*, 4128–4136.
39. Sykiotis, G.P., Plummer, L., Hughes, V.A., Au, M., Durrani, S., Nayak-Young, S., Dwyer, A.A., Quinton, R., Hall, J.E., Gusella, J.F., et al. (2010). Oligogenic basis of isolated gonadotropin-releasing hormone deficiency. Proc. Natl. Acad. Sci. USA *107*, 15140–15144.
40. Shaw, N.D., Seminara, S.B., Welt, C.K., Au, M.G., Plummer, L., Hughes, V.A., Dwyer, A.A., Martin, K.A., Quinton, R., Mericq, V., et al. (2011). Expanding the phenotype and genotype of female GnRH deficiency. J. Clin. Endocrinol. Metab. *96*, E566–E576.
41. Chan, Y.M., Broder-Fingert, S., Paraschos, S., Lapatto, R., Au, M., Hughes, V., Bianco, S.D., Min, L., Plummer, L., Cerrato, F., et al. (2011). GnRH-deficient phenotypes in humans and mice with heterozygous variants in KISS1/Kiss1. J. Clin. Endocrinol. Metab. *96*, E1771–E1781.
42. Gianetti, E., Tusset, C., Noel, S.D., Au, M.G., Dwyer, A.A., Hughes, V.A., Abreu, A.P., Carroll, J., Trarbach, E., Silveira, L.F., et al. (2010). TAC3/TACR3 mutations reveal preferential activation of gonadotropin-releasing hormone release by neurokinin B in neonatal life followed by reversal in adulthood. J. Clin. Endocrinol. Metab. *95*, 2857–2867.
43. Adzhubei, I.A., Schmidt, S., Peshkin, L., Ramensky, V.E., Gerasimova, A., Bork, P., Kondrashov, A.S., and Sunyaev, S.R. (2010). A method and server for predicting damaging missense mutations. Nat. Methods *7*, 248–249.
44. Kumar, P., Henikoff, S., and Ng, P.C. (2009). Predicting the effects of coding non-synonymous variants on protein function using the SIFT algorithm. Nat. Protoc. *4*, 1073–1081.
45. Ferrer-Costa, C., Orozco, M., and de la Cruz, X. (2004). Sequence-based prediction of pathological mutations. Proteins *57*, 811–819.
46. Schwarz, J.M., Rödelsperger, C., Schuelke, M., and Seelow, D. (2010). MutationTaster evaluates disease-causing potential of sequence alterations. Nat. Methods *7*, 575–576.
47. Reese, M.G., Eeckman, F.H., Kulp, D., and Haussler, D. (1997). Improved splice site detection in Genie. J. Comput. Biol. *4*, 311–323.
48. Lage, K., Hansen, N.T., Karlberg, E.O., Eklund, A.C., Roque, F.S., Donahoe, P.K., Szallasi, Z., Jensen, T.S., and Brunak, S. (2008). A large-scale analysis of tissue-specific pathology and gene expression of human disease genes and complexes. Proc. Natl. Acad. Sci. USA *105*, 20870–20875.
49. Lage, K., Karlberg, E.O., Størling, Z.M., Olason, P.I., Pedersen, A.G., Rigina, O., Hinsby, A.M., Tümer, Z., Pociot, F., Tommerup, N., et al. (2007). A human phenome-interactome network of protein complexes implicated in genetic disorders. Nat. Biotechnol. *25*, 309–316.
50. Lage, K., Møllgård, K., Greenway, S., Wakimoto, H., Gorham, J.M., Workman, C.T., Bendsen, E., Hansen, N.T., Rigina, O., Roque, F.S., et al. (2010). Dissecting spatio-temporal protein networks driving human heart development and related disorders. Mol. Syst. Biol. *6*, 381.
51. Karin, M. (1995). The regulation of AP-1 activity by mitogen-activated protein kinases. J. Biol. Chem. *270*, 16483–16486.
52. Raivio, T., Sidis, Y., Plummer, L., Chen, H., Ma, J., Mukherjee, A., Jacobson-Dickman, E., Quinton, R., Van Vliet, G., Lavoie, H., et al. (2009). Impaired fibroblast growth factor receptor 1 signaling as a cause of normosmic idiopathic hypogonadotropic hypogonadism. J. Clin. Endocrinol. Metab. *94*, 4380–4390.
53. Pitteloud, N., Quinton, R., Pearce, S., Raivio, T., Acierno, J., Dwyer, A., Plummer, L., Hughes, V., Seminara, S., Cheng, Y.Z., et al. (2007). Digenic mutations account for variable phenotypes in idiopathic hypogonadotropic hypogonadism. J. Clin. Invest. *117*, 457–463.
54. Meyers, E.N., Lewandoski, M., and Martin, G.R. (1998). An Fgf8 mutant allelic series generated by Cre- and Flp-mediated recombination. Nat. Genet. *18*, 136–141.
55. Tsai, P.S., Moenter, S.M., Postigo, H.R., El Majdoubi, M., Pak, T.R., Gill, J.C., Paruthiyil, S., Werner, S., and Weiner, R.I. (2005). Targeted expression of a dominant-negative fibroblast growth factor (FGF) receptor in gonadotropin-releasing hormone (GnRH) neurons reduces FGF responsiveness and the size of GnRH neuronal population. Mol. Endocrinol. *19*, 225–236.
56. Correia, K.M., and Conlon, R.A. (2001). Whole-mount in situ hybridization to mouse embryos. Methods *23*, 335–338.
57. Kovalenko, D., Yang, X., Nadeau, R.J., Harkins, L.K., and Friesel, R. (2003). Sef inhibits fibroblast growth factor signaling by inhibiting FGFR1 tyrosine phosphorylation and subsequent ERK activation. J. Biol. Chem. *278*, 14087–14091.
58. Torii, S., Kusakabe, M., Yamamoto, T., Maekawa, M., and Nishida, E. (2004). Sef is a spatial regulator for Ras/MAP kinase signaling. Dev. Cell *7*, 33–44.
59. Chan, Y.M., de Guillebon, A., Lang-Muritano, M., Plummer, L., Cerrato, F., Tsiaras, S., Gaspert, A., Lavoie, H.B., Wu, C.H., Crowley, W.F., Jr., et al. (2009). GNRH1 mutations in patients with idiopathic hypogonadotropic hypogonadism. Proc. Natl. Acad. Sci. USA *106*, 11703–11708.
60. Francou, B., Bouligand, J., Voican, A., Amazit, L., Trabado, S., Fagart, J., Meduri, G., Brailly-Tabard, S., Chanson, P., Lecomte, P., et al. (2011). Normosmic congenital hypogonadotropic hypogonadism due to TAC3/TACR3 mutations: characterization of neuroendocrine phenotypes and novel mutations. PLoS ONE *6*, e25614.
61. Quaynor, S.D., Kim, H.G., Cappello, E.M., Williams, T., Chorich, L.P., Bick, D.P., Sherins, R.J., and Layman, L.C. (2011). The prevalence of digenic mutations in patients with normosmic hypogonadotropic hypogonadism and Kallmann syndrome. Fertil. Steril. *96*, 1424–1430, e6.
62. Topaloglu, A.K., Reimann, F., Guclu, M., Yalin, A.S., Kotan, L.D., Porter, K.M., Serin, A., Mungan, N.O., Cook, J.R., Ozbek, M.N., et al. (2009). TAC3 and TACR3 mutations in familial hypogonadotropic hypogonadism reveal a key role for Neurokinin B in the central control of reproduction. Nat. Genet. *41*, 354–358.
63. White, B.J., Rogol, A.D., Brown, K.S., Lieblich, J.M., and Rosen, S.W. (1983). The syndrome of anosmia with hypogonadotropic hypogonadism: a genetic study of 18 new families and a review. Am. J. Med. Genet. *15*, 417–435.
64. Mason, I., Chambers, D., Shamim, H., Walshe, J., and Irving, C. (2000). Regulation and function of FGF8 in patterning of midbrain and anterior hindbrain. Biochem. Cell Biol. *78*, 577–584.
65. Kawauchi, S., Shou, J., Santos, R., Hébert, J.M., McConnell, S.K., Mason, I., and Calof, A.L. (2005). Fgf8 expression defines a morphogenetic center required for olfactory neurogenesis and nasal cavity development in the mouse. Development *132*, 5211–5223.
66. Tucker, E.S., Lehtinen, M.K., Maynard, T., Zirlinger, M., Dulac, C., Rawson, N., Pevny, L., and Lamantia, A.S. (2010). Proliferative and transcriptional identity of distinct classes of neural

precursors in the mammalian olfactory epithelium. Development *137*, 2471–2481.
67. Lin, W., Fürthauer, M., Thisse, B., Thisse, C., Jing, N., and Ang, S.L. (2002). Cloning of the mouse Sef gene and comparative analysis of its expression with Fgf8 and Spry2 during embryogenesis. Mech. Dev. *113*, 163–168.
68. Storm, E.E., Rubenstein, J.L., and Martin, G.R. (2003). Dosage of Fgf8 determines whether cell survival is positively or negatively regulated in the developing forebrain. Proc. Natl. Acad. Sci. USA *100*, 1757–1762.
69. Waldstreicher, J., Seminara, S.B., Jameson, J.L., Geyer, A., Nachtigall, L.B., Boepple, P.A., Holmes, L.B., and Crowley, W.F., Jr. (1996). The genetic and clinical heterogeneity of gonadotropin-releasing hormone deficiency in the human. J. Clin. Endocrinol. Metab. *81*, 4388–4395.
70. Pirvola, U., Ylikoski, J., Trokovic, R., Hébert, J.M., McConnell, S.K., and Partanen, J. (2002). FGFR1 is required for the development of the auditory sensory epithelium. Neuron *35*, 671–680.
71. Mortensen, O.V. (2013). MKP3 eliminates depolarization-dependent neurotransmitter release through downregulation of L-type calcium channel Cav1.2 expression. Cell Calcium *53*, 224–230.
72. Thisse, B., and Thisse, C. (2005). Functions and regulations of fibroblast growth factor signaling during embryonic development. Dev. Biol. *287*, 390–402.
73. Alsina, F.C., Irala, D., Fontanet, P.A., Hita, F.J., Ledda, F., and Paratcha, G. (2012). Sprouty4 is an endogenous negative modulator of TrkA signaling and neuronal differentiation induced by NGF. PLoS ONE *7*, e32087.
74. Hausott, B., Vallant, N., Schlick, B., Auer, M., Nimmervoll, B., Obermair, G.J., Schwarzer, C., Dai, F., Brand-Saberi, B., and Klimaschewski, L. (2012). Sprouty2 and -4 regulate axon outgrowth by hippocampal neurons. Hippocampus *22*, 434–441.
75. Yamagishi, S., Hampel, F., Hata, K., Del Toro, D., Schwark, M., Kvachnina, E., Bastmeyer, M., Yamashita, T., Tarabykin, V., Klein, R., and Egea, J. (2011). FLRT2 and FLRT3 act as repulsive guidance cues for Unc5-positive neurons. EMBO J. *30*, 2920–2933.
76. Tata, B.K., Chung, W.C., Brooks, L.R., Kavanaugh, S.I., and Tsai, P.S. (2012). Fibroblast growth factor signaling deficiencies impact female reproduction and kisspeptin neurons in mice. Biol. Reprod. *86*, 119.
77. Lin, W., Jing, N., Basson, M.A., Dierich, A., Licht, J., and Ang, S.L. (2005). Synergistic activity of Sef and Sprouty proteins in regulating the expression of Gbx2 in the mid-hindbrain region. Genesis *41*, 110–115.